

A Pattern Language for Machine Learning Tasks

Benjamin Rodatz
Computer Science, Oxford,
Quantinuum

Ian Fan
Jump Trading, London

Tuomas Laakkonen
MIT

Neil John Ortega
Quantinuum

Thomas Hoffmann
Aridis AG

Vincent Wang-Maścianica
HAILab, Philosophy, Oxford

Abstract

We formalise the essential data of objective functions as equality constraints on composites of learners. We call these constraints "tasks", and we investigate the idealised view that such tasks determine model behaviours. We develop a flowchart-like graphical mathematics for tasks that allows us to;

1. offer a unified perspective of approaches in machine learning across domains;
2. design and optimise desired behaviours model-agnostically;
3. import insights from theoretical computer science into practical machine learning.

As a proof-of-concept of the potential practical impact of our theoretical framework, we exhibit and implement a novel "manipulator" task that minimally edits input data to have a desired attribute. Our model-agnostic approach achieves this end-to-end, and without the need for custom architectures, adversarial training, random sampling, or interventions on the data, hence enabling capable, small-scale, and training-stable models.

Contents

1	Introduction	2	5	Concluding discussion	18
1.1	Contributions	3	5.1	Summary	18
2	Tasks and patterns	4	5.2	Relation to extant work	18
2.1	Tasks	4	5.3	Limitations and Prospects	19
2.2	Patterns are "nice" tasks	5	A	String diagrams for tasks	25
2.3	Analysing complex tasks	5	A.1	Task diagram semantics	25
2.4	Proof of concept: Stacks	7	A.2	Universal approximator semantics . . .	26
3	The manipulation task	8	B	Strong manipulation	29
3.1	Theoretical analysis	9	C	Experiment Details	30
3.1.1	Proof: Bayesian inversion	9	C.1	Spriteworld	30
3.1.2	Proof: CycleGAN	11	C.2	Faces	31
4	Experimental validation of manipulator	14	C.3	MNIST	31
4.1	Simple attributes	14	D	Manipulation in complex domains	33
4.2	Derived Attributes	16	D.1	Manipulation for text sentiment	33
4.3	Interpretability applications	17	D.2	Manipulation as generative classifier .	35

1 Introduction

The primary instrument for controlling the training of machine learning (ML) models is the objective function, which can be broken into three modular parts. Let Θ_e, Θ_d be the parameter-spaces of a model enc and dec respectively. Then the reconstruction loss that characterises an autoencoding task amounts to minimising (for $\theta_e \in \Theta_e, \theta_d \in \Theta_d$) the following objective function:

$$\operatorname{argmin}_{\theta_e, \theta_d} (\mathbb{E}_{x \sim \mathcal{X}} [\mathbf{D}(\mathbf{dec}_{\theta_d}(\mathbf{enc}_{\theta_e}(x)), x)])$$

We take the **expected value** over a **data distribution** \mathcal{X} of a **measure of statistical divergence** \mathbf{D} (such as cross-entropy or log-likelihood) of **two expressions** that, **under ideal conditions, should be equal**: the decoding of the encoding of some data x , and the original x . In this work, we focus on the two expressions that want to be equal, and we call this **equational constraint** a *task*.

In practice, designing a good objective function incorporates many technical choices, such as choice of architecture, measure of statistical divergence, and training data [17, 58, 65]. However, these choices are often made by heuristics, or rationalised post hoc. While such choices are sometimes required to make training tractable, they are not always relevant to understanding the final behaviour of the trained model. Instead, we propose and investigate the idealised view that:

Tasks determine model behaviour.

Unpacking this bird's eye perspective of deep learning for a mathematical audience, the view we propose is that deep learning is nonlinear representation theory: instead of linear maps representing groups, smooth maps represent higher algebraic structures such as coloured PROPs [72] for typed function composition, and the role of gradient descent is to convert data and compute into instances of these functorial representations.

Unpacking the same perspective as a value proposition for practitioners, we suggest that just as physicists connect mathematical equations to physical reality, we can design AI systems by writing down task equations that capture what we want them to do in terms we understand, and then we let neural networks and gradient descent figure out how to satisfy those equations by themselves.

To reason about tasks compactly, we use flowchart-like string diagram notation.

Example 1.1. For a hyperparameter choice of divergence \mathbf{D} , where X is an input datatype, and LAT is the datatype of the latent space, the two components of the empirical risk minimisation of the autoencoder *task* consist of (1) applying the encoder enc (typed $X \rightarrow LAT$) followed by the decoder dec (typed $LAT \rightarrow X$) to inputs x drawn from a source of data \mathcal{X} over the datatype X , *which should be equal to* (2) the original x . We depict this as:

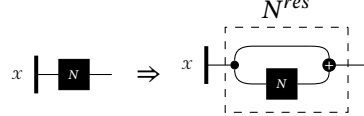
$$\mathbb{E}_{x \sim \mathcal{X}} [\mathbf{D}(\underbrace{\mathbf{dec}_{\theta_d}(\mathbf{enc}_{\theta_e}(x))}_{(1)}, \underbrace{x}_{(2)})] \quad x \xrightarrow{\mathbf{enc}} \underbrace{\mathbf{LAT}}_{\mathbf{dec}_{\theta_d}(\mathbf{enc}_{\theta_e}(x))} \xrightarrow{\mathbf{dec}} x \quad \xrightleftharpoons{\mathbf{enc}, \mathbf{dec}} \quad x \xrightarrow{\mathbf{enc}, \mathbf{dec}} x$$

The diagrammatic notation is formally equivalent to the traditional symbolic notation with the addition of type-information about inputs and outputs. While the formal details (Appendix A) involve category theory, the power of string diagrams lies in their intuitive visual nature: by reading the diagrams as flowcharts from left to right, practitioners can leverage these diagrams to reason about ML tasks without needing to fully grasp the underlying mathematical formalism. In summary, nodes depicted as various shapes are functions, and wires are datatypes which can be understood as carrying information.

To explore the expressive power of tasks, **we abstract away implementation details such as architecture and training by idealising models to be universal function approximators** that can, in principle, perfectly optimise objective functions. Thus each task can be viewed purely as an equational constraint on the behaviour of the learners, comparable to equational constraints on the possible values of variables in algebra. **This perspective allows us two ways to specialise tasks by imposing structural inductive biases**, by specifying architectural choices, or by adding additional objectives. Specifying tasks can be used to increase trainability or to add additional, desirable restrictions/behaviours.

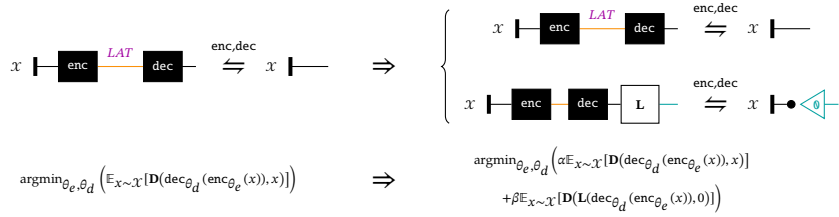
Example 1.2 (Residuation as an architectural choice). One example of an architectural specification is adding a residual to a learner. Diagrammatically, choosing an architecture means substituting a "black-box" universal

function approximator with another diagram with matching input-output type constraints; intuitively, since a universal function approximator can be any function, it can *in particular* be a specific function of the same input-output type if necessary. The formal semantics for such substitutions are provided in Appendix A.2. A simple example is residuation, where a learner N of type $X \rightarrow X$ is transformed into $N^{res} := x \mapsto N(x) + x$, depicted as:



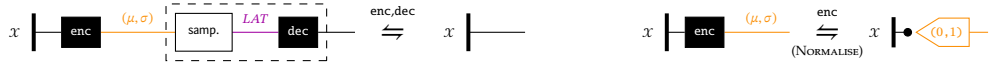
While from the abstract lens of universal function approximators, adding a residual should not affect the expressiveness of a learner, in practice, we might observe improved trainability.

Example 1.3 (Perceptual losses as multi-objective learning). An example of task specification is adding perceptual loss to an autoencoder. A common form of multi-objective learning is to add a normalisation or regularisation term to an objective function, for instance, a perceptual loss $\mathbf{L} : X \rightarrow \mathbb{R}^{\geq 0}$ (which we depict with a "white box", because there are no learnable parameters). Multiple tasks may be combined into single objective functions by means of weighted summation with positive hyperparameter-coefficients α, β .



Specialisation of tasks obtains desirable properties without compromising basic behaviours, and allows us to explain the behaviour of models in terms of their constituent tasks. As a canonical example, we may obtain a variational autoencoder (VAE) [41] from a regular one by the two kinds of specialisation described.

Example 1.4 (VAE). Setting the output type of the encoder to be a space (mean, variance) of parameters for Gaussians; declaring the decoder to be internally structured as the sequential composite of sampling from a Gaussian of the input (mean, variance) followed by a learner; adding an additional normalisation task which requires the outputs of the encoder to be close to $(0, 1)$ — the parameters of the unit Gaussian. enc maps the input space X to (μ, σ) , the parameter-space of Gaussians over the latent space LAT . The decoder is the composite of a sampling function $\text{samp.} : (\mu, \sigma) \rightarrow LAT$ and a learner $\text{dec} : LAT \rightarrow X$. Note the additional NORMALISE task that enc must satisfy. This presentation of VAEs is equivalent to the traditional probabilistic form when the statistical divergence is KL [59].



1.1 Contributions

We make three primary contributions in this work. Our first, theoretical contribution is **the formalisation of a common but informal standard procedure in deep learning**, which may be summarised as the following recipe:

1. Characterise desired behavior via equational constraints (tasks) between learners
2. Implement tasks by treating neural networks as universal approximators
3. Convert equations to loss function by a choice of hyperparameters, namely weighted sum of constituent losses and choice of divergences

Our second, theoretical contribution is a demonstration that **using our framework, we may analyse, predict, and design behaviours of models**. Using specialisation and algebraic reasoning, we can analyse the behaviour of complex models in terms of simple, well-understood tasks we call *patterns*. Moreover,

we can define a novel synthetic relationship between tasks called *refinement* which describes when one optimally trained set of tasks entails satisfaction of a different set of tasks. Altogether, we may use these techniques to understand and compare the behaviour of models before committing to potentially costly training. Example 2.6 and Propositions 2.11, 3.6 and 3.11 illustrate the kinds of formal reasoning our language enables.

Our third, practical contribution and proof-of-concept is the **implementation of a novel problem class we call manipulation** (Section 3), which formalises [5] the problem of viewing and editing a targeted attribute of data while "leaving other aspects the same". Notably, this task represents the first problem class to our knowledge that appears to be naturally solved by the relatively underexplored technique of "multi-learner multi-objective learning", which our framework naturally accommodates. As examples in image domains, we; change only the colour of a shape (Figure 2); change the value of a handwritten digit without affecting other stylistic properties (Figure 3); and change only whether a person is smiling in an image (Figure 7). Even in these toy domains, we observe a range of benefits we expect to scale: by following our recipe we obtain architecture-agnostic (Table 1) style-transference models without the need for randomness, adversarial training, or modality- and architecture-specific interventions, with good interpolation properties (Figure 7).

We conclude by discussing relations to similar approaches in the literature, along with avenues and prospects for further development.

2 Tasks and patterns

2.1 Tasks

We assume the following contextual data, omitted if there is no confusion. Let X, Y denote datatypes; Σ a set of processes f , each of which has (possibly empty) learnable parameter datatypes \mathfrak{p}_f . An atomic task is a process-theoretic equational constraint on learners specifying that f should behave like g on all inputs. The objective function of an atomic task φ of type $X \rightarrow Y$ equipped with distribution \mathcal{X} corresponds to a map $\mathfrak{p}_\varphi \rightarrow \mathbb{R}$ that sends $\pi \mapsto \mathbb{E}_{x \sim \mathcal{X}}[\mathbf{D}(\text{sys}_{\varphi; \pi}(x), \text{spec}_{\varphi; \pi}(x))]$ for some choice of statistical divergence \mathbf{D} . A learner can optimise multiple atomic tasks simultaneously by optimising a combination α of the atomic objective functions (commonly obtained by taking a weighted sum).

Definition 2.1 (Tasks). An *atomic task* φ is a tuple $(f, g, \mathcal{X}, \mathfrak{p})$, where $f, g : X \rightarrow Y$ are composite processes of Σ , \mathcal{X} is a distribution over X , and $\mathfrak{p} \subseteq \mathfrak{p}_f \oplus \mathfrak{p}_g$ is a space of trainable parameters. We indicate the *system* f and *specification* g as sys_φ and spec_φ and similarly the *domain* X and *codomain* Y as $\text{dom}(\varphi)$ and $\text{cod}(\varphi)$. A *compound task* Φ (or just *task*) is a non-empty set of tasks. As we have seen in previous examples, we denote a task Φ as a collection of atomic tasks $\text{sys}_\varphi \leftrightharpoons \text{spec}_\varphi$, where superscripts on the harpoons indicate which learnable parameters are governed by each atomic task.

Tasks become concrete objective functions by a hyperparametric choice of divergences for atomic tasks, followed by a combination via a weighted sum with hyperparameter coefficients, or more generally a *compound function*. As such, a particular objective function that instantiates a task is one where the choices for the measure of statistical divergence and compound function have been made. Beyond these hyperparameters, tasks and objective functions may be viewed as informationally equivalent.

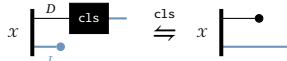
Definition 2.2 (Objective function). Let $\Phi = \{(f_i, g_i, \mathcal{X}_i, \mathfrak{p}_i)\}_{i \in N}$ be a compound task with N atomic tasks. Let $l \in \Sigma$ be a learner of Φ . An *objective function* for l is a tuple $(\Phi_l, \mathcal{D}, \alpha)$ where $\Phi_l = \{(f_i, g_i, \mathcal{X}_i, \mathfrak{p}_i) \mid \text{para}(l) \subseteq \mathfrak{p}_i\}$ is the set of all tasks on which l is optimised, \mathcal{D} is a set of *statistical divergences* $\mathbf{D}_{(\varphi \in \Phi_l)} : \text{cod}(\varphi) \times \text{cod}(\varphi) \rightarrow \mathbb{R}^{\geq 0}$, and the *compound function* α is a function $(\mathbb{R}^{\geq 0})^{\times |\Phi_l|} \rightarrow \mathbb{R}^{\geq 0}$ that is differentiable, and typically non-decreasing in each argument.

To illustrate these definitions, throughout the following sections, we will show an abundance of tasks and relate them to their respective objective functions.

2.2 Patterns are "nice" tasks

We do not expect there to be a general and systematic method to translate between natural-language behavioural specifications and tasks; if such a method existed, then all of deep learning would be reduced to hyperparameter search. There are often many different ways to approach a problem in ML, much like there is no single correct way to write software, or design a building. This suggests to us the view of *patterns*: some tasks are well understood, usable modularly and in many contexts, and easily modifiable, and such tasks can be viewed as *design patterns* – borrowing a term from software engineering [6]¹. In this section, we suggest some examples of patterns that correspond to well-studied methods and paradigms in ML, and we show how to use **patterns as an accessible basis to analyse models**.

Pattern 2.3 (classification).



Given a data-label pair (d, l) drawn from \mathcal{X} with labels $l \in \mathcal{L}$, a *classifier* $\text{cls} : D \rightarrow \mathcal{L}$ is a function that solves the *classification* task, in which it seeks to reconstruct the label from the data. This can be done by minimising the corresponding objective function $\mathbb{E}_{(d, l) \sim \mathcal{X}}[\mathbf{D}(\text{cls}(d), l)]$ for some measure of statistical divergence \mathbf{D} on the label space, which may be continuous to encompass regression.

Pattern 2.4 (autoencoding).



As we have seen, given a data distribution \mathcal{X} over X and some latent space LAT , an *autoencoder* consists of an *encoder* $\text{enc} : X \rightarrow LAT$ and a *decoder* $\text{dec} : LAT \rightarrow X$ which cooperate to reconstruct the identity over the observed distribution, by minimising $\mathbb{E}_{x \sim \mathcal{X}}[\mathbf{D}(\text{dec}(\text{enc}(x)), x)]$.

Pattern 2.5 (GAN). Given a data distribution \mathcal{X} over X and noise distribution \mathcal{N} over N , a *generative adversarial network* (GAN) consists of a *generator* $\text{gen} : N \rightarrow X$ and a *discriminator* $\text{dsc} : X \rightarrow [0, 1]$. The prosaic explanation that "the discriminator seeks to distinguish real data from fake data while the generator aims to fool the discriminator" translates directly into a task description: where 1 indicates "real" and 0 indicates "fake", the discriminator dsc seeks to minimise some positive combination of the terms $\mathbb{E}_{x \sim \mathcal{X}}[\mathbf{D}(\text{dsc}(x), 1)]$ and $\mathbb{E}_{x \sim \mathcal{X}}[\mathbf{D}(\text{dsc}(\text{gen}(x)), 0)]$, while the generator gen seeks to minimise $\mathbb{E}_{x \sim \mathcal{X}}[\mathbf{D}(\text{dsc}(\text{gen}(x)), 1)]$.

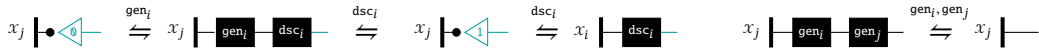


For the sake of compactness, on the right hand side, we compressed the two adversarial tasks into one figure where the discriminator and generator pull into opposite directions.

2.3 Analysing complex tasks

We can analyse the intended functions of models by viewing them as composites of simple patterns. We have already seen in Example 1.4 how a VAE is analysable by inspection as a specialised regular autoencoder. As a second example, a CycleGAN is two GANs on different distributions, whose generators are mutually autoencoders by a *cycle consistency loss* [73]. This suggests that the generators encode the distributions into each other in a reversible manner, and indeed this kind of style transfer between distributions is what a CycleGAN does in practice.

Example 2.6 (CycleGAN). Below, i, j are nonequal indices taking values in $\{0, 1\}$, where \mathcal{X}_0 and \mathcal{X}_1 are different distributions on the same space X : typically these are two classes of images.



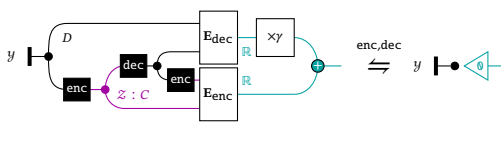
Tasks allow us to reason "legalistically" to rule out undesirable model behaviours. For instance, in Example 1.4, we can immediately determine that the normalisation term imposes a nontrivial constraint: without the normalisation task, enc and dec could collude against us by only using variance 0 (i.e.

¹And before that, architecture and urban design [2].

deterministic) representations that are far apart, which would lose the ease of sampling and robustness of representations. We further elaborate on the use of this form of reasoning for informing task design in Appendix B.

We can also upgrade informal intuitions into formal derivations. For example, on the account of [57], a broad class of unsupervised learning techniques — including PCA and k -means — are specialisations of the energy minimisation task, which may be considered an autoencoding task from a latent "code" space subject to the representations minimising a measure of "energy". We can in fact formalise the relationship between these forms of unsupervised learning and autoencoding, showing that under mild assumptions, they are the same in the computational limit.

Pattern 2.7 (energy minimisation).



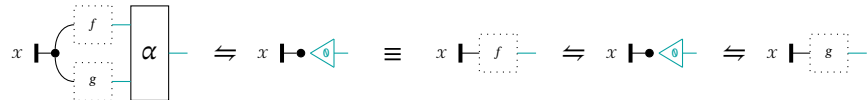
energy minimisation consists of; three types of systems: $D(\text{ata})$, $C(\text{ode})$, and $\mathbb{R}^{\geq 0}$; two learnable processes: an encoder $\text{enc} : D \rightarrow C$ and a decoder $\text{dec} : C \rightarrow D$; two user-supplied *energy functions*: $\mathbf{E}_{\text{enc}} : C \times C \rightarrow \mathbb{R}^{\geq 0}$ and $\mathbf{E}_{\text{dec}} : D \times D \rightarrow \mathbb{R}^{\geq 0}$; and a user-supplied constant $\gamma \in \mathbb{R}^{\geq 0}$. Provided a distribution of inputs \mathcal{Y} on D , and a distribution \mathcal{Z} on C the system seeks to minimise $\mathbb{E}_{y \sim \mathcal{Y}, z \sim \mathcal{Z}}[\gamma \mathbf{E}_{\text{enc}}(\text{enc}(y), z) + \mathbf{E}_{\text{dec}}(y, \text{d}(z))]$. Such a task is called *code-extracting* when $\mathcal{Z} = \text{enc}(\mathcal{Y})$.

To formally relate code-extracting energy minimisation and autoencoding, we introduce a relationship between tasks called *refinement*, which states that perfectly solving Φ allows one to construct perfect solutions for Ψ . When Φ and Ψ refine each other, the tasks are "the same in the computational limit"; a perfect autoencoder is a perfect code-extracting energy minimiser, and vice versa. These relationships are a proxy for the behaviour and relative power of concrete implementations of tasks.

Definition 2.8 (Refinement and equivalence of tasks). Task Φ *refines* task Ψ if, by treating the atomic tasks as equations, the processes of Φ may be composed to satisfy the equations of Ψ . Φ and Ψ are *equivalent* if they refine one another, which we denote $\Phi \equiv \Psi$.

Now we aim to prove that autoencoders and energy-minimisers are identical in the computational limit: that a "perfect" deterministic autoencoder yields a "perfect" energy-minimiser, and vice versa.

Lemma 2.9. For all well-typed f, g , and for any positive linear combination $\alpha : \mathbb{R}^{\geq 0} \times \mathbb{R}^{\geq 0} \rightarrow \mathbb{R}^{\geq 0}$:



Proof. For the forward refinement, as α is a positive linear combination, we have for all $x \in \mathcal{X}$ that $\alpha(f(x), g(x)) = \alpha_1 \cdot f(x) + \alpha_2 \cdot g(x) = \mathbf{0}$. If f and g are constant-functions 0, we are done. Otherwise, positivity implies that $\alpha_1 \cdot f(x) = \alpha_2 \cdot g(x) = \mathbf{0}$, and since $\alpha_1, \alpha_2 \in \mathbb{R}^{\geq 0}$, then $f(x) = \mathbf{0} = g(x)$, which is the desired task. For the backwards refinement, if $f(x) = \mathbf{0} = g(x)$ for all $x \in \mathcal{X}$, then $\alpha(f(x), g(x)) = \alpha_1 \cdot f(x) + \alpha_2 \cdot g(x) = \mathbf{0}$. \square

Lemma 2.10. For a real-valued pairwise measure $\mathbf{D} : \mathcal{D}(Y) \times \mathcal{D}(Y) \rightarrow \mathbb{R}^{\geq 0}$ on the space of distributions over Y , the positivity axiom $\mathbf{D}(\mathcal{Y}_1, \mathcal{Y}_2) = 0 \iff \mathcal{Y}_1 = \mathcal{Y}_2$ implies, for (almost²) all $f, g : X \rightarrow Y$ and \mathcal{X} :

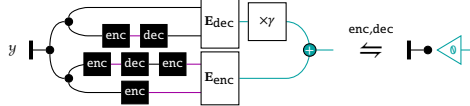


Proof. For the forward refinement, we assume that $\mathbf{D}(f(\mathcal{X}), g(\mathcal{X})) = \mathbf{0}$. By positivity of \mathbf{D} , $f(\mathcal{X}) = g(\mathcal{X})$, which is the right hand task. For the backward refinement, if $f(\mathcal{X}) = g(\mathcal{X})$, then, by positivity, $\mathbf{D}(f(\mathcal{X}), g(\mathcal{X})) = \mathbf{0}$. \square

Proposition 2.11. If enc and dec are deterministic and \mathbf{E}_{enc} and \mathbf{E}_{dec} are positive (e.g. metrics or statistical divergences), then energy minimisation \equiv autoencoding.

²When the function space containing f and g is large, the edge case where f and g are nonconstant and $f = -g$ is measure-theoretically negligible. Since we are concerned with behaviour in the computational limit, this is an acceptable assumption for our purposes.

Proof. As enc and dec are functions, we may copy them through their outputs to re-express energy minimisation as:



By Lemma 2.9, this is equivalent to:



Recall that E_{enc} and E_{dec} are positive by definition, hence Lemma 2.10 allows us to express the two minimisations as:

$$y \vdash \xrightarrow{\text{enc,dec}} y \vdash \text{enc} \text{ dec} \vdash \quad y \vdash \text{enc} \text{ dec} \text{ enc} \vdash \xrightarrow{\text{enc,dec}} y \vdash \text{enc} \vdash$$

The left task is autoencoding, so we have that energy minimisation refines autoencoding. For the other direction, we observe that autoencoding refines the right task by postcomposing both sides with enc , and as the left and right tasks together are equivalent to energy minimisation, we have the claim. \square

2.4 Proof of concept: Tasks from specifications - the stack

In this section and the following (Section 3), we will provide two examples of utilising the proposed perspective to design new tasks. First, we will propose and experimentally verify a set of tasks that restrain two interacting learners to perform the *push* and *pop* operations of a stack. While by itself the stack is not particularly interesting, this section is more used as a first introduction to working with tasks to create desired behaviour. In Section 3 we will introduce a more involved tasks for manipulating attributes in data.

The well-known data structure stack consists of two interacting operations: *push* and *pop*.

Task 2.12 (stack). Given a data distribution \mathcal{X} over X and a pretrained autoencoder ($\text{enc}: X \rightarrow \text{LAT}$, $\text{dec}: \text{LAT} \rightarrow X$), a stack consists of a *empty stack* $\perp : \star \rightarrow S$, a push operation $\text{psh} : S \times X \rightarrow S$ and a pop operation $\text{pop} : S \rightarrow S \times X$. We recursively define the distribution:

$$\mathcal{D} := \perp \times \text{enc}(\mathcal{X}) \quad | \quad \text{psh}(d \in \mathcal{D}, x \in \mathcal{X}) \times \text{enc}(x)$$

meaning \mathcal{D} is a stack of arbitrary size and an encoded element from \mathcal{X} .

Then *psh* and *pop* have to obey the following rules:



For completeness, and to illustrate the ergonomic necessity of our diagrammatic notation, we display the formulaically obtained hyperparameterised objective function of stack in standard notation below. The appeal of the diagrammatic notation will become even more obvious in Section 3.

$$\text{argmin}_{\phi, \psi} \left(\underbrace{\alpha \mathbf{D}_1(\text{pop}_\phi(\perp), (\perp, 0))}_{\text{EMPTY}} + \underbrace{\beta \mathbb{E}_{(s,x) \sim \mathcal{D}} [\mathbf{D}_2(\text{pop}_\phi(\text{push}_\psi(s, x)), (s, x))]}_{\text{PSHPOP}} \right)$$

Where ϕ, ψ, χ are the parameters of *push*, *pop* and \perp to be learnt; α, β are hyperparametric positive weighting coefficients for each task; $\mathbf{D}_1, \mathbf{D}_2$ are hyperparametric statistical divergences for $S \times X$.

Given the purely demonstrational role of this experiment, we will do a proof-of-concept on a simple analytic dataset (Figure 2) inspired by Spriteworld [69] consisting of images depicts a single shape with varying properties. We observe that the stack works exactly as expected (see Figure 1).

While the basic stack task is not particularly interesting, it does provide a fully differentiable data structure which may be useful in composite with other tasks.

"Stacks" methodology: This experiment uses an autoencoder architecture for processing 32×32 RGB images, with a latent space size of 16 dimensions. The encoder consists of four convolutional layers, each with 64 channels and a channel multiplier of 1. Additionally, a stack of 64 latent features is processed through an MLP with 256 hidden units. Training is performed on a GPU, with a batch size of 64, learning rate of 1×10^{-4} , weight decay of 1×10^{-2} , and gradient clipping at 1. The model trains for 100,000 steps, logging every 10,000 steps. Input images are converted to tensors and scaled to floating-point precision, and a fixed random seed of 0 ensures reproducibility. The stack space S has to be n times larger than the latent space Lat for the stack to be able to hold up to n items.

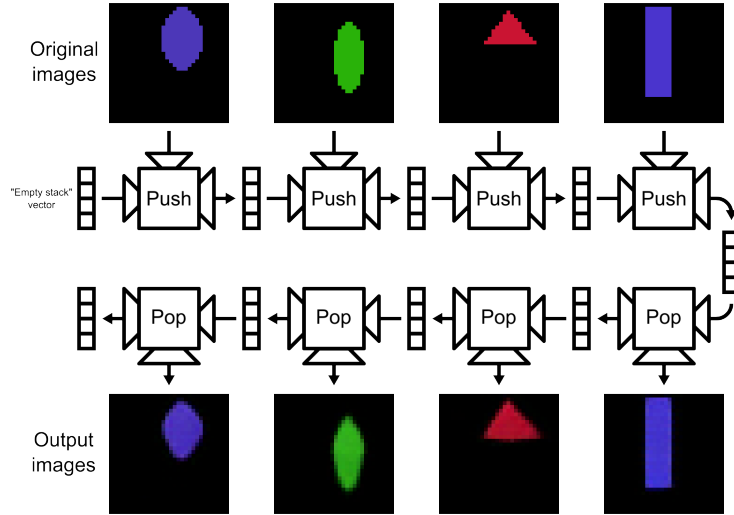


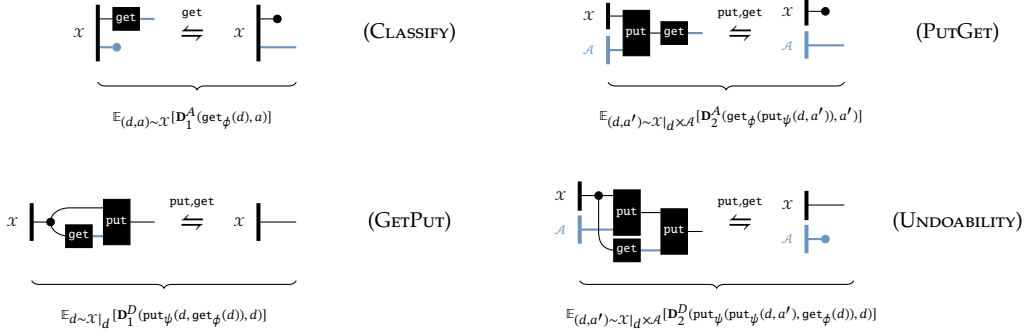
Figure 1: In this example, we train a stack (alongside an autoencoder) to store the latent vectors of Spriteworld shapes. With an image latent size 16 and stack vector size 64, it is able to retain information to faithfully restore up to 4 shapes.

3 The manipulation task

In this section, we design and theoretically analyse **manipulation**, a novel task which aims to view and edit a property of data without explicit guidance. In Section 4, we will experimentally validate the task. There are many models that behave like manipulators, e.g. unsupervised sentiment translation [43, 63] in the text domain and prompt-based photo editing [35, 39] in the image domain. While most of these approach this question on the architectural level to impose the desired behaviour, we will instead approach this problem via the objective function - constraining the learning process. To constrain the behaviour of manipulation, we demonstrate another ability of our framework: importing insights from computer science more broadly via the process-theoretic perspective. For manipulation, we reference the field of Bidirectional Transformations, which studies consistency between different overlapping representations of data [1]. A special case is the view-update problem [5] originally proposed for databases: how do we algebraically characterise reading-out and updating an attribute $a \in A$ from some data $d \in D$? There are a family of solutions called *lenses* which are parameterised by algebraic laws of varying strength [48], which we take inspiration from below:

Task 3.1 (manipulation). Let $\mathcal{X} : (d, a)$ be a distribution over some data $d \in D$, each labelled with an attribute $a \in A$ and let \mathcal{A} be a distribution over the attributes. A **manipulation** consists of a pair of operations ($\text{get} : D \rightarrow A$, $\text{put} : D \times A \rightarrow D$) which can be understood as reading and writing, respectively. In particular, the **put** edits a reference data point to exhibit the specified attribute. The two operations have to obey the

following tasks, with respect to the modeller’s choice of distribution \mathcal{A} on A .



To provide an intuition for each of the tasks, assume that the data consists of images each containing a single shape each labeled with the colour of the shape. **CLASSIFY** allows us to use **get** to read out the colour of a shape. **PUTGET** says that first editing the colour of a shape (say, from red to blue) and then immediately reading out that colour will return the edited colour (blue). **GETPUT** says that reading out the colour of a shape (say, red) followed by editing the shape to have the same colour (i.e., an edit that leaves red unchanged) is the same as doing nothing. **UNDOABILITY** says that edits can be undone; using the first **put** to change the colour of a shape (say from red to blue), and then editing again with a second **put** to restore the original, read-out colour of the shape (red) must restore the original image.

Once again, for completeness, we display the hyperparameterised objective function of **manipulation** in standard notation below:

$$\text{argmin}_{\phi,\psi} \left(\underbrace{\alpha \mathbb{E}_{(d,a) \sim \mathcal{X}} (\mathbf{D}_1^A (\text{get}_\phi(d), a)) + \beta \mathbb{E}_{(d,a') \sim \mathcal{X} \mid d \times \mathcal{A}} (\mathbf{D}_2^A (\text{get}_\phi(\text{put}_\psi(d, a')), a'))}_{\text{CLASSIFY}} \right. \\ \left. + \underbrace{\gamma \mathbb{E}_{d \sim \mathcal{X} \mid d} (\mathbf{D}_1^D (\text{put}_\psi(d, \text{get}_\phi(d)), a)) + \delta \mathbb{E}_{(d,a') \sim \mathcal{X} \mid d \times \mathcal{A}} (\mathbf{D}_2^D (\text{put}_\psi(\text{put}_\psi(d, a'), \text{get}_\phi(d)), d))}_{\text{PUTGET}} \right) \\ \left. + \underbrace{\mathbb{E}_{(d,a') \sim \mathcal{X} \mid d \times \mathcal{A}} (\mathbf{D}_1^D (\text{put}_\psi(d, \text{get}_\phi(d)), a')) + \mathbb{E}_{(d,a') \sim \mathcal{X} \mid d \times \mathcal{A}} (\mathbf{D}_2^D (\text{put}_\psi(\text{put}_\psi(d, a'), \text{get}_\phi(d)), d))}_{\text{UNDOABILITY}} \right)$$

Where ϕ, ψ are the parameters of **put** and **get** to be learnt; $\alpha, \beta, \gamma, \delta$ are hyperparametric positive weighting coefficients for each task; $\mathbf{D}_1^A, \mathbf{D}_2^A$ are hyperparametric statistical divergences for A ; $\mathbf{D}_1^D, \mathbf{D}_2^D$ are statistical divergences for D ; and \mathcal{A} is a hyperparametric distribution over A such that $\text{supp}(\mathcal{A})$ contains the attributes the modeller intends to have as targets.

3.1 Theoretical analysis

Beyond providing an intuitive language for objective functions, the proposed diagrammatic language can also be used to prove properties about a particular choice of objective function. In this section, we will prove two facts about the **manipulator** that let us make predictions about its most likely behaviour after training.

First, we argue that the idealised form of the **manipulator** — in which attribute information is fully disentangled from the rest of the data — is inherently challenging to realise in practice. This is because, in complex data domains, isolating and inverting attribute-specific structure often entails recovering detailed, latent factors of variation. Such a disentangled inversion effectively requires the system to act as a conditional generator that precisely modifies only the attribute of interest while leaving all other features unchanged.

Despite this, we still expect the **manipulator** to perform well in realistic settings. Specifically, we show that the manipulation objective refines the structure of a **CycleGAN**, meaning that — under ideal training — it should match or exceed the behavioural guarantees of a standard **CycleGAN** system. Whether such performance is actually achieved in practice depends on empirical training success, which we investigate in Section 4.

3.1.1 Proof 1 - Bayesian inversion

In the ideal case, the **manipulator** would completely separate the information about the attribute it is manipulating from all other information. If it managed to do this, it could manipulate exactly the attribute

while leaving everything else as is. For this to be possible, there must exist a complement datatype C such that our original data distribution \mathcal{D} can be separated into two independent distributions \mathcal{A} and \mathcal{C} . Assuming that this is possible, we will show that (a) being able to do such a separation would freely give a **manipulator** and (b) that this **manipulator** would refine **Bayesian inversion**, a task that is known to be difficult for complex data domains.

First, we define:

Definition 3.2 (Balanced entropy of an attribute). Given a distribution of data \mathcal{D} on space D , we say that a distribution \mathcal{A} over space A represents an *entropy-balanced attribute* of \mathcal{D} if there exists a complement type C with distribution \mathcal{C} such that we have the equality in distributions $\mathcal{D} = \mathcal{C} \times \mathcal{A}$ up to an isomorphism of the underlying spaces $D \simeq (C \times A)$.

If there exists such an isomorphism, then we know that there must exist two functions that observe the isomorphism. We have:

Definition 3.3 (Latent split autoencoder). Let the attribute A induce a balance attribute on some distribution \mathcal{D} . Then the functions $enc : \mathcal{D} \rightarrow \mathcal{C} \times \mathcal{A}$ and $dec : \mathcal{D} \rightarrow \mathcal{C} \times \mathcal{A}$ that observe this isomorphism between the two underlying spaces satisfy the following three conditions:

$$\mathcal{D} \xrightarrow{D} \text{enc} \xrightarrow{C} \text{dec} \xrightarrow{A} \mathcal{D} \xrightleftharpoons{enc, dec} \mathcal{D} \xrightarrow{D} \mathcal{D} \quad (1)$$

$$\mathcal{A} \xrightarrow{A} \text{dec} \xrightarrow{C} \text{enc} \xrightarrow{A} \mathcal{A} \xrightleftharpoons{enc, dec} \mathcal{A} \xrightarrow{A} \mathcal{A} \quad (2)$$

$$\mathcal{D} \xrightarrow{D} \text{enc} \xrightarrow{C} \mathcal{D} \xrightleftharpoons{enc} \mathcal{D} \xrightarrow{D} \text{cls} \xrightarrow{C} \mathcal{D} \quad (3)$$

The two functions are suggestively named *enc* and *dec* as the first condition indeed specifies that they have to act as an autoencoder on \mathcal{D} . We will show that given such an idealised autoencoder, we can freely, i.e. without any additional training, create a **manipulator**:

Proposition 3.4 (Manipulator from latent split autoencoder). Let \mathcal{D} be a distribution with a balanced attribute A . Then a **latent split autoencoder** refines **manipulator**.

Proof. We can define:

$$\begin{array}{c} \mathcal{D} \xrightarrow{D} \text{put} \xrightarrow{A} \mathcal{D} \\ := \quad \begin{array}{c} \mathcal{D} \xrightarrow{D} \text{enc} \xrightarrow{C} \text{dec} \xrightarrow{A} \mathcal{D} \\ \text{---} \end{array} \end{array} \quad \begin{array}{c} \mathcal{D} \xrightarrow{D} \text{get} \xrightarrow{A} \mathcal{D} \\ := \quad \begin{array}{c} \mathcal{D} \xrightarrow{D} \text{enc} \xrightarrow{C} \mathcal{D} \\ \text{---} \end{array} \end{array}$$

We now have to show that this is indeed a **manipulator**.

For this, we show that the *put* and *get* observe the restrictions of the manipulator:

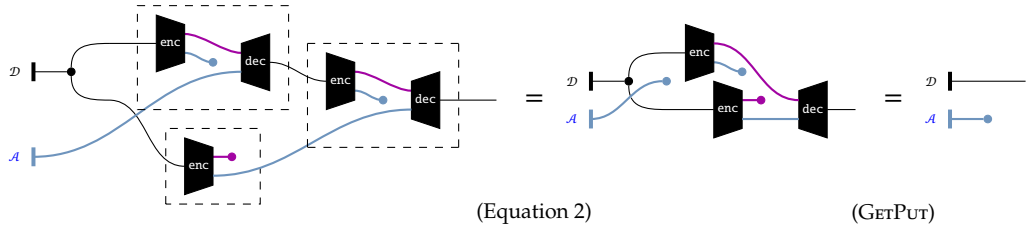
PutGet:

$$\begin{array}{c} \mathcal{D} \xrightarrow{D} \text{enc} \xrightarrow{C} \text{dec} \xrightarrow{A} \mathcal{D} \\ \text{---} \end{array} = \begin{array}{c} \mathcal{D} \xrightarrow{D} \text{enc} \xrightarrow{C} \mathcal{D} \\ \text{---} \end{array} = \begin{array}{c} \mathcal{D} \xrightarrow{D} \bullet \\ \text{---} \end{array} \quad \begin{array}{c} \text{(Equation 2)} \\ \text{(Delete naturality)} \end{array}$$

GetPut:

$$\begin{array}{c} \mathcal{D} \xrightarrow{D} \bullet \xrightarrow{C} \text{enc} \xrightarrow{C} \text{dec} \xrightarrow{A} \mathcal{D} \\ \text{---} \end{array} = \begin{array}{c} \mathcal{D} \xrightarrow{D} \text{enc} \xrightarrow{C} \text{dec} \xrightarrow{A} \mathcal{D} \\ \text{---} \end{array} = \begin{array}{c} \mathcal{D} \xrightarrow{D} \text{enc} \xrightarrow{C} \text{dec} \xrightarrow{A} \mathcal{D} \\ \text{---} \end{array} = \begin{array}{c} \mathcal{D} \xrightarrow{D} \text{enc} \xrightarrow{C} \text{dec} \xrightarrow{A} \mathcal{D} \\ \text{---} \end{array} \quad \begin{array}{c} \text{(copy naturality)} \\ \text{(copy-delete counitality)} \\ \text{(autoencoder)} \end{array}$$

UNDOABILITY:



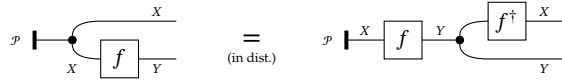
□

Thus, solving the information separation problem would also give a solution to the manipulator.

We will now show that this is difficult by proving that this manipulator freely provides a Bayesian inversion to a classifier from D to A .

We define:

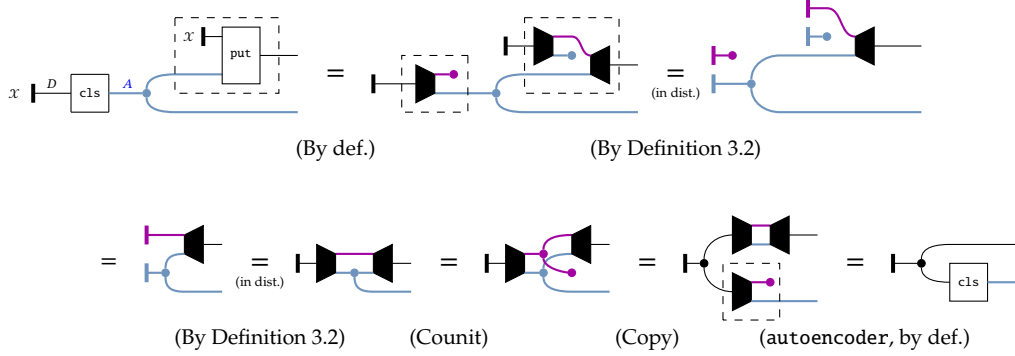
Definition 3.5 (Bayesian Inversion in Markov Categories). The Bayesian inversion [15, 50] of a stochastic map $f : X \rightarrow Y$ with respect to a distribution \mathcal{P} on X is a stochastic map $f^\dagger : Y \rightarrow X$ such that, in distribution:



We can show:

Proposition 3.6 (Manipulator as Bayesian inversion). If a discriminative classifier $\text{cls} : D \rightarrow A$ induces a balanced attribute $\text{cls}(\mathcal{D})$ over A with respect to D , then the manipulator specified above refines Bayesian inversion $\text{cls}^\dagger : A \rightarrow D$.

Proof. We show that the put composed with an independent copy of the data source \mathcal{X} is the Bayesian inversion of cls .



1

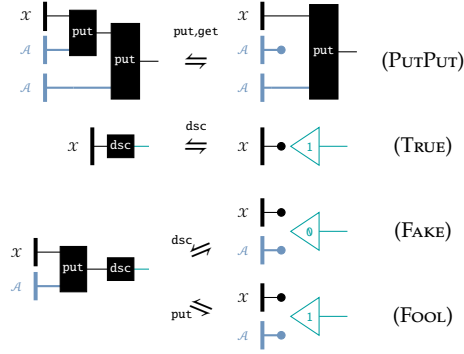
As such we have shown that the idealised solution to the manipulation problem would also give a solution to Bayesian inversion - a problem that is known to be hard [cite](#). Therefore, one might question why we expect this setup to succeed. Before giving empirical proof, we will first give a theoretical intuition by relating manipulation to the known task of CycleGAN.

3.1.2 Proof 2 - CycleGAN

CycleGANs (Example 2.6) solve a similar task as manipulation, translating between two distributions. In fact, with the additional regularisation terms, strong manipulation is a refinement of CycleGAN, giving us more guarantees by avoiding certain failure cases. We can use the pattern language to show this formally.

To show this relationship, we have to add additional regularisation terms to the manipulation task. While these are theoretically justified (see Appendix B), in practice they are less train stable. Therefore, in Section 4, we will use the vanilla manipulator as a starting point.

Task 3.7 (strong manipulation add-ons).



The PUTPUT task (which, paired with PUTGET and GETPUT is strictly stronger than UNDOABILITY in that it is algebraically implied) says that the effect of putting twice is the same as discarding the effect of the first edit and only keeping the last edit. In conjunction with PUTGET and GETPUT, this creates what is known in the literature as a *very well-behaved lens*.

The TRUE, FAKE, and FOOL tasks introduce a discriminator component dsc , which forms a GAN pattern with respect to put as the generator. When well-trained, this forces the outputs of put to lie in-distribution. As in general there are no algebraic or equational laws that characterise arbitrary distributions of data, using GANs in this way is a generic recipe for shaping outputs of generators to behave well in-distribution.

With these new regularisation term, the manipulator is not perfectible anymore, as, by design, it is impossible for the put and the dsc to have a loss of zero at the same time. Therefore, we have to generalise the definition of *refinement* to *partially perfectible tasks*.

Definition 3.8 (Partially perfectible task). A *partially perfectible task* $\{(f_i, g_i, \mathcal{X}_i, \mathfrak{p}_i)\}_i$ with learnable functions Σ_l is a compound task with excluded learners $E \subseteq \Sigma_l$ such that:

1. no two $e \in E$ share atomic tasks, i.e. $\forall e, e' \in E. \{(f_i, g_i, \mathcal{X}_i, \mathfrak{p}_i) | e \in f_i \vee e \in g_i\} \cap \{(f_i, g_i, \mathcal{X}_i, \mathfrak{p}_i) | e' \in f_i \vee e' \in g_i\} = \emptyset$ and
2. all tasks not involving learners from E are perfectible, i.e. $\exists \pi \in \mathfrak{p}. \forall x \in X. f_{i;\pi}(x) = g_{i;\pi}(x)$

Importantly, there does not need to exist a perfect solution for all tasks. As condition (1) explicitly forbids excluded learners to share tasks, we do not need to make restrictions on their composite behaviour.

For any task, we can define partially perfectible (sub-)tasks. A trivial partially perfectible task is when excluding all learners. A more interesting example is CycleGAN with excluded learners dsc_1, dsc_2 . Assuming an appropriate data distribution [71], the autoencoding tasks, i.e. the reconstruction losses, are perfectible. The generator-discriminator tasks, which are not perfectible, are not included, as we explicitly exclude the learners for the discriminators. This means that for this partially perfectible task, we only care about the training results of the two generators and do not care about the discriminators.

When we have partially perfectible tasks, we have to define what we mean by an optimal solution.

Definition 3.9 (Optimal partially perfect solution). Let $\Phi = \{(f_i, g_i, \mathcal{X}_i, \mathfrak{p}_i)\}_i$ be a partially perfectible tasks with learners Σ and excluded learners $E \subseteq \Sigma$. Then an *optimal partially perfect solution* for the learners $L = \Sigma \setminus E$ is, if it exists, a set of parameters $\pi_L \in \mathfrak{p}_L$ such that for a given $\alpha_L, \mathbf{D}_\phi$ they

- perfect the tasks that do not include any excluded learners
- for the tasks that include excluded learners, the included learners are optimal, meaning there exists no other set of parameters for the included learners whose worst-case performance against some parameterization of the excluded learners is better

Clearly, such a partially perfect solution may not always exist, either because there is no solution that is optimal for the included tasks given the choice of $\alpha_L, \mathbf{D}_\phi$ or as there may be more optimal solutions for the non-perfectible tasks that do not satisfy the perfectible tasks.

Given this, we can generalise the definition of *refinement* for partially perfectible tasks.

Definition 3.10 (Optimal refinement of partially-perfectible tasks). Given two partially-perfectible tasks Ψ, Φ with excluded learners E_Ψ, E_Φ , we say that Ψ optimally refines Φ if optimal partially perfect solutions for $\Sigma_{l_\Psi} \setminus E_\Psi$ can be composed to form optimal partially perfect solutions for $\Sigma_{l_\Phi} \setminus E_\Phi$.

For $A_\Psi, A_\Phi = \emptyset$, optimal refinement is equivalent to refinement.

To show that **strong manipulation** optimally refines CycleGAN, we need one assumption: we assume that the measure of statistical divergence and compound function have been chosen such that a generator in a generative-adversarial setting is optimal if and only if its output distribution is equal to the original distribution. As the goal of such a generative setting is to approximate the original distribution, this is quite a natural assumption. One possible choice of measure of statistical divergence and compound function that has been proven to fulfil this assumption is given by Goodfellow et al. [32, Theorem 1].

Proposition 3.11 (Manipulation vs. Style-transfer). Given appropriately chosen measure of statistical divergence and compound functions, **strong manipulation** with excluded learner `dsc` optimally refines CycleGAN with excluded learners `dsc1`, `dsc2`.

Proof. Let $\mathcal{X}_1, \mathcal{X}_2$ be two distributions over the same type. We create $\mathcal{X} = (x, i)$ for $x \in \mathcal{X}_i$ where the label i indicates the distribution the data point came from. Assuming that we have `(get, put, disc)` that satisfy **strong manipulation** with an optimal partially perfect `put`, `get`, we can construct optimal partially perfect generators G_1 and G_2 for CycleGAN.

For $i \in 0, 1, j = 1 - i$, we define:

$$\xrightarrow{G_1} := \xrightarrow{\text{put}}$$

First, we show that the perfectible tasks are indeed perfected, i.e. that both the autoencoder tasks are fulfilled. We have:

$$\begin{aligned} x_j \xrightarrow{G_i} G_j &= x_j \xrightarrow{\text{put}} \text{put} &= x_j \xrightarrow{\text{put}} \text{put} \\ &\quad (\text{Def}) && \quad (\text{PutPut}) \\ &= x_j \xrightarrow{\text{get}} \text{put} &= x_j \xrightarrow{\text{put}} \\ &\quad (\text{Classify}) && \quad (\text{GetPut}) \end{aligned}$$

Next, we will show that these generators are indeed globally optimal. By assumption, a generator is optimal if and only if its output distribution is indistinguishable from the training distribution. Thus, assuming that the components of manipulation are optimal with respect to the generative-adversarial tasks, `put` output distribution approaches $\mathcal{X} = (x, i)$ for $x \in \mathcal{X}_i$. But by `PutGet`, we have:

$$\begin{aligned} x_j \xrightarrow{G_i} \text{get} &= x_j \xrightarrow{\text{put}} \text{get} &= x_j \xrightarrow{\text{put}} \text{get} \\ &\quad (\text{Def}) && \quad (\text{PutGet}) \end{aligned}$$

Therefore, by `CLASSIFY`, G_1 and G_2 can only return values that are akin to values in \mathcal{X}_1 and \mathcal{X}_2 respectively. As these two labels make up the entirety of \mathcal{X} , G_1 's and G_2 's output distributions are indistinguishable from \mathcal{X}_1 and \mathcal{X}_2 respectively. Therefore, they are indeed optimal generators for their respective distribution.

But then we have shown that G_1 and G_2 are indeed optimal solutions to CycleGAN and therefore that manipulation is a specialisation of CycleGAN³. \square

In turn, CycleGAN, however, is not a refinement of **strong manipulation**. This means there exist solutions to CycleGAN, which violate **strong manipulation**. In these image translation tasks, we expect the translators to change as little as possible to go from one distribution to the other, i.e. preserving as much information from the original as possible. However, the generators of CycleGAN could, for example, flip the images horizontally. As the autoencoder-like tasks have an even number of generators on each side, this would be a ‘perfect solution’ to the outlined task, yet not the behaviour we would want or expect. In contrast, the `PutPut` rule of **strong manipulation** does not allow this behaviour. As such, **strong manipulation** gives us more guarantees than CycleGAN.

Despite the additional guarantees, **strong manipulation** does not guarantee that it indeed only changes as little as necessary to go from one distribution to the other. To showcase this, we will consider a degenerate

³In [73], when doing style transfer, they additionally add the *identity loss* which enforces that generating an image in X_i given an image from X_1 should return the identity. This perfectible task is also guaranteed by **strong manipulation** by `cls` and `GetPut`.

example, where it becomes obvious that no unique solution to the `manipulator` can exist. Considering the following toy scenario: the data has the four objects *circle*, *square*, *red* and *green*. There is no unique mapping between shapes and colours. Without further information, it is therefore completely impossible to say what it would mean to change as little as possible to go from shapes to colours. It becomes obvious that, without specifying further restrictions on all remaining attributes, it is impossible to know which mapping is correct. Yet, despite these theoretical concerns, in practice, even `manipulator` often converges to the desired behaviour, similar to CycleGAN, which has even fewer guarantees.

4 Experimental validation of `manipulator`

Beyond the theoretical results about the `manipulator`, we will show experimental validation of its performance. For this, we will first provide some toy examples of the vanilla `manipulator`, a setting in which we can also adapt it to distributions without balanced entropy. Finally, we will showcase the `manipulator` with more realistic data, manipulating attributes of faces. For technical implementation details, see Appendix C.

4.1 Experimental Results I: Simple attributes of synthetic and real-world data

We first demonstrate initial proofs-of-concept of the `manipulation` task on a simple analytic dataset (Figure 2) inspired by Spriteworld [69], and on MNIST (Figure 3). In the former, each image depicts a single shape with varying properties, and is labelled by two attributes: shape – circle, square or triangle – and colour – red, green or blue. For each attribute, we train a `get`/`put` pair according to the `manipulation` task specification.

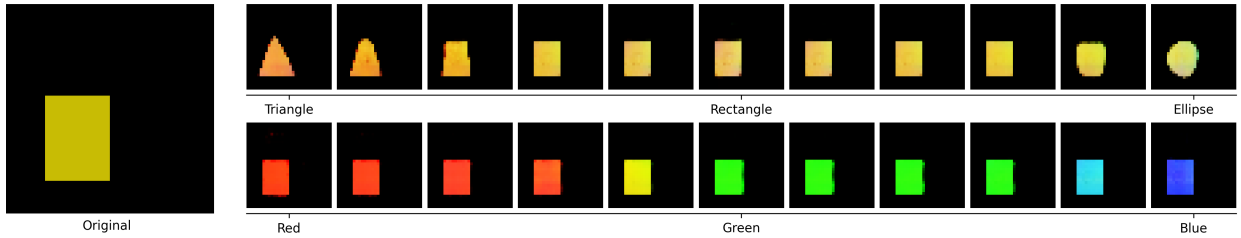


Figure 2: An input Spriteworld image alongside a spectrum of outputs exhibiting the ability of the `put` to manipulate a single attribute of the input while preserving its other properties. Additionally, the model is able to generalise by interpolating to attribute values unseen during training, in this case producing orange and cyan shapes, whereas during training, it only sees red, green or blue shapes. (further details in Section C.1)

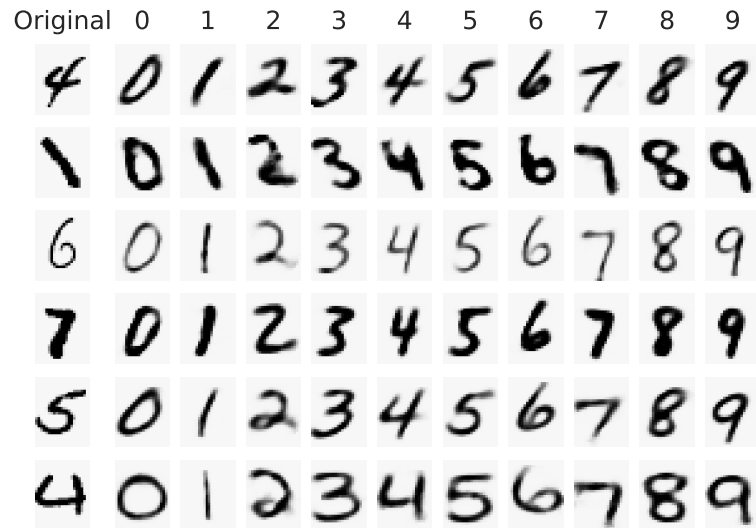


Figure 3: Outputs of a put trained against an MNIST classifier. The put preserves several graphological aspects, such as stroke weight, slant, and angularity. This represents qualitative evidence to support our prediction that put as a class-conditioned generative model behaves as a style-preserving edit.

4.2 Experimental Results II: Derived attributes of synthetic data

Often in practice we are interested in complex, non-explicit attributes that are derived from those labelled in the data: for example, "eligibility for a loan" may be derived from other explicit attributes of people in a database by an operationally opaque classifier, with unknown range, distribution, and dependencies on other attributes. A known challenge in manipulating derived attributes is unequal entropy in attribute classes [16], which may cause models such as CycleGANs to hide data imperceptibly, making them particularly vulnerable to adversarial attacks. Various solutions have been proposed, including masks [71], blurring [30] and compression [23]. We demonstrate via a modification of manipulation (Task 3.1, Figure 5) that **our framework permits the design and implementation of end-to-end approaches to editing complex attributes without interventions on the data.**

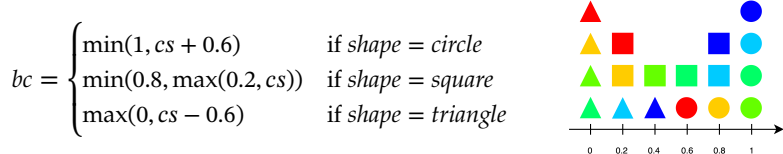


Figure 4: To illustrate the concepts of derived attributes and unequal entropy, consider an attribute on the Spriteworld data called *blue-circleness*, which broadly measures how similar a shape is to a blue circle. We define *blue-circleness* (bc) as a function of explicit attributes $shape$ and $colour$; we assign a continuous colour score $cs \in [0, 1]$ based on the hue, where red = 0 and blue = 1. To illustrate unequal entropy in this example, the class 0 has higher entropy than 0.4 because there are more shapes that have bc -value 0. So manipulating a shape with bc -value 0 to 0.4 must lose information.

Task 4.1 (complement manipulation).

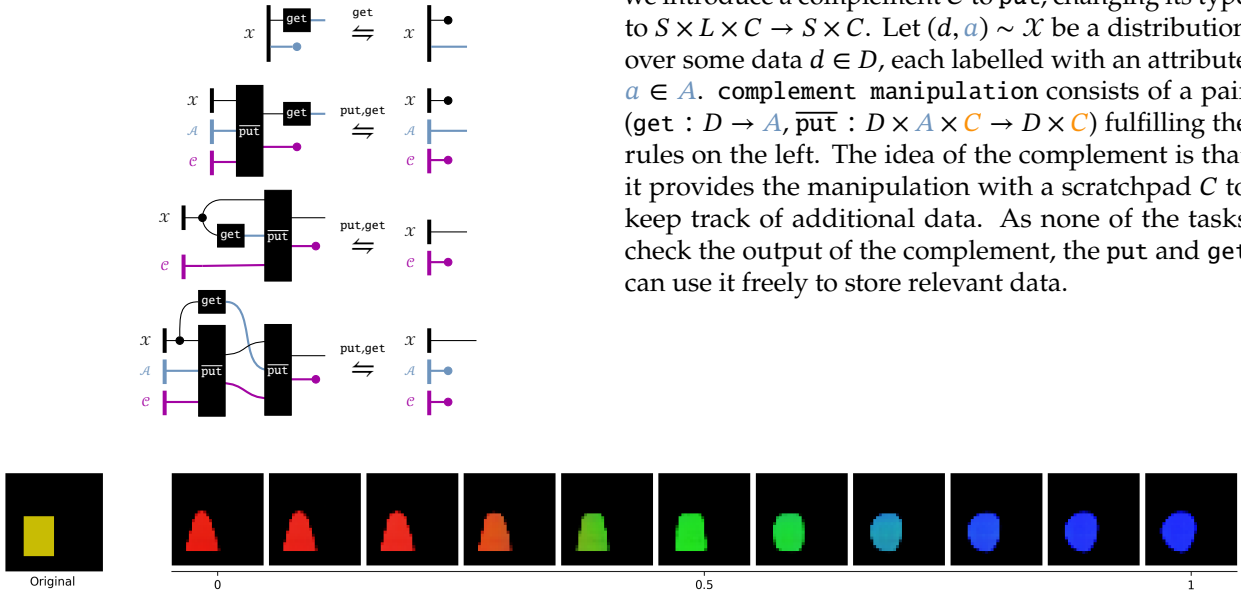


Figure 5: Complement manipulators (Task 4.1) can manipulate derived attributes such as *blue-circleness*, by using the complement as a scratchpad to record a correspondence between data points (further details in Section C.1) while preserving attributes such as position and size.

4.3 Experimental results III: Interpretability applications on real-world data

As a further test of the robustness of tasks to implementation choices, we specialised the `put` to be a simple vector addition in the latent space of an autoencoder (Figure 6), for the relatively complex *Large-scale CelebFaces Attributes* dataset. We found that restricting `put` to be linear in this way increased training stability. Moreover, in the same way that we would expect a latent space "filtered through" the probabilistic structure of Gaussians to yield good sampling properties (Example 1.4), we would predict that enforcing linear structure on the latent space would yield "linear" properties. Indeed, we exhibit continuous interpolation in generated outputs between normally discrete class labels (Figure 7), and class-sensitive separation of latent space embeddings in the autoencoder. We consider this to be compelling evidence that **since our framework is agnostic, implementation details may be engineered to obtain additional desirable properties without compromising behavioural specifications.**

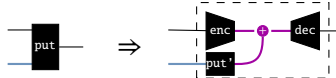


Figure 6: Recalling that architectural choices are a form of specialisation by diagrammatic substitution, the linear `put` is a specialisation of a generic `put` as an autoencoder task-bound pair of learners `enc` and `dec`, along with a `put'` that computes single shift vector to be added into the latent space, depending only on the label value. `enc`, `dec`, and `put'` are trained simultaneously along with the manipulation tasks, and intuitively this pressures the autoencoder pair to adapt their latent representations to fit the needs of the broader manipulation task.

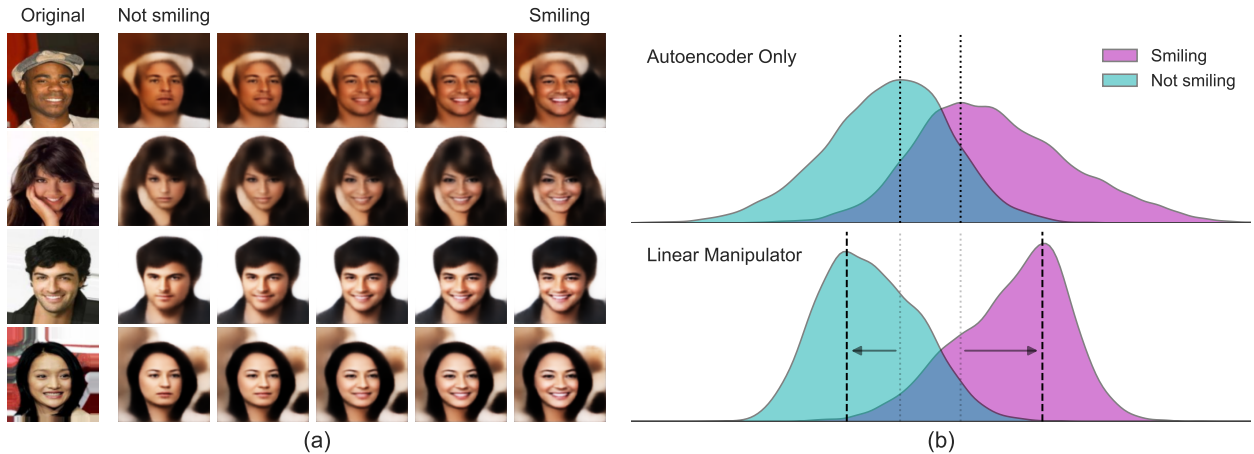


Figure 7: *Left:* Outputs of a linear manipulator trained on face image data paired with a binary "smile"/"no-smile" label. The remarkable aspect of this experiment is that the original data only carried binary smile/no-smile labels, and that the linear structure in the specialisation of the `put` admits continuous interpolation. *Right:* A comparison of the spread of the latent embeddings of images from the validation set when pre-training an autoencoder and then training a (linear) classifier on the latent space (top), vs. when trained with a linear manipulator (bottom). We find that linear `put` automatically separates latent space embeddings of classes: the graphs depict the relative density of embeddings along the direction of the classifiers' weight vectors, normalised so that each combined data spread is centred and has unit variance (details in Section C.2).

5 Concluding discussion

5.1 Summary

We introduced a diagrammatic language for representing and reasoning about the behaviour of machine learning models in terms of tasks, viewed as the essential data of objective functions. By leveraging category theory and string diagrams, our work establishes a cross-disciplinary formal bridge between theoretical computer science and practical machine learning, providing new conceptual tools for analyzing ML systems and permitting the transfer of insights between traditionally separate fields.

The proposed framework allows capturing existing tasks in machine learning, providing intuitive insights rooted in mathematical rigour. We identify a set of widespread and well-understood tasks, which we call patterns. We can analyse some tasks as composites of patterns (Example 2.6) while other tasks can be understood as specialisations of patterns (Example 1.4). The rewrite system inherent to string diagrams, allows us to identify relationships between different tasks and formalise intuitions (Proposition 2.11, Proposition 3.11).

Beyond theoretical insights, the proposed language also allows the creation of new training paradigms. As preliminary empirical validation of our theory’s utility and potential, we introduced a novel task type called `manipulator` that produces a class-conditioned and style-preserving generative model counterpart for a given classifier. In the image domain, we were able to verify predicted behaviours (Section 4.1), and we demonstrated the ability to design novel end-to-end capabilities, such as end-to-end editing of complex attributes (Section 4.2) and the imposition of linear structure on latent space representations (Section 4.3), which allowed continuous interpolation between discrete class labels on real data, and separated latent space embeddings of different classes. Notably, this was achieved without adversarial training conditions, random sampling, preprocessing of data, or hardcoded interventions in the architectures, i.e.:

Our framework enables capable, small-scale, and training-stable models.

5.2 Relation to extant work

Regarding our nascent theoretical framework as a whole, the style of engineering beginning from tasks is already common practice in many fields of ML, and we sought here to place these practices on a more rigorous footing, and to probe their strengths and limitations. Our mathematical approach draws broadly from the field of Applied Category Theory [24], particularly in the use of string diagrams for the higher-algebraic data of concurrently and serially composed functions, which enables compact representation and reasoning with otherwise cumbersome symbolic equivalents when dealing with multiple learners in tandem. To our knowledge, our concern with the composition of tasks among many learners distinguishes our aims and formal choices from approaches that employ similar mathematical formulations, both within the category-theoretic literature (cf. [31]), and without (cf. the variational generalisation of Bayesian inference presented in [42]).

While our approach is essentially neurosymbolic in spirit, it does not fit neatly into the mainstream triad of neurosymbolic approaches [22]; we do not encode symbolic data for neural operations, nor do we interface neural approaches with symbolic engines, nor are we hardcoding expert knowledge representations. Moreover, our aims differ: while neurosymbolic approaches often seek to manipulate symbolic data systematically by neural means, our framework operates at a higher level of abstraction, seeking to use the systematicity of higher-algebraic equational characterisations as a means to shape the neural ends. Hence our perspective may complement existing approaches to structure in machine learning.

Regarding `manipulation` in particular, this was to our knowledge the first practically demonstrated synthesis of insights from Bidirectional Transformations as a subfield of database theory [1] with ML. While explicitly neurosymbolic approaches have been tried for similar editing tasks before (see e.g. [61]), owing to the influence of database theory in our approach, to our knowledge our statement and execution of this task enjoys the maximal permissible generality and implementation agnosticism among similar attribute-editing tasks, without sacrificing rigour and systematicity.

5.3 Limitations and Prospects

Concerning `manipulation` in particular, an immediately evident limitation of this practical demonstration is a lack of exploration of how the difficulty of training such ensembles of learners behaves at scale, with respect to more complex and multimodal datasets, and with a wider range of architectures. Concerning scale, while none of the products of our experimentation are state-of-the-art with respect to specific applications, we believe the variety and promise of these results serve as a compelling validation of our theoretical framework's utility and potential. Concerning applications of `manipulator` beyond the image domain, we report on some sketch experiments in sentiment-manipulation on text in Appendix D, where we also comment on the nature of technical difficulties to be overcome in the application of the `manipulator` to complex domain data, and offer an explanation for mode collapses observed during training by empirically relating `manipulator` to other generative classification approaches. Concerning a wider range of architectures, we report on some specialisations of the learners. However, we leave exploring `manipulation` in combination with state-of-the-art architectures, such as diffusion, for future work.

Addressing the theoretical framework of tasks more broadly, our reliance on equational characterisations is double-edged. On one hand, it is uncommon to find such characterisations of mathematical systems of interest as they are usually defined by more direct means, and this presents a theoretical limitation. On the other hand, it appears that the strength of equational characterisations when applied to ML lies in imposing structure on "the way to learn to solve a problem" rather than on the solutions or problems themselves [64]. This suggests promising future possibilities of our mathematical framework in bridging structural-symbolic approaches from computer science more broadly with methods that can effectively leverage computation. For example, the toy-example of the "neural data structure" of the `stack` might be a first step in this direction (see Section 2.4).

While we have demonstrated that, in certain cases, tasks can determine behaviours, there is a theoretical gap in the converse analysis of behaviours of trained models in terms of their basic tasks. The problem is typified by generative models where it is impossible a priori for all of the constituent tasks to be simultaneously perfectly optimised. The prototypical illustrating example is the GAN, where it is impossible for both the generator and discriminator to be perfect. Conceptually, the gap is that we have only dealt here with "static" ensembles which in principle admit idealised loss-minimisations, whereas some generative models use adversarial tasks to enforce "dynamic" training forces for a variety of purposes, such as representation regularisation for easier sampling in VAEs. While we do offer some initial methods of analysis in subsubsection 3.1.2, a more thorough and encompassing analysis is beyond the scope of this paper.

Future theoretical developments will seek to incorporate other aspects of ML: for example, relating to work that focuses on the choice of model architecture [40] and interactions with the underlying data distribution [14]. While our current experiments focus on demonstrating our framework's validity, future practical developments will explore applications to more complex, real-world ML challenges, where we envision our approach informing areas such as AutoML, interpretable AI, and formal verification of ML systems: the compositional nature of our task-based framework naturally aligns with neural architecture search by potentially informing principled search strategies for optimal model architectures, and the explicit representation of model behaviours as equational constraints could enhance interpretability and facilitate formal verification.

References

- [1] Faris Abou-Saleh, James Cheney, Jeremy Gibbons, James McKinna, and Perdita Stevens. *Introduction to Bidirectional Transformations*, pages 1–28. Springer International Publishing, Cham, 2018. ISBN 978-3-319-79108-1. doi: 10.1007/978-3-319-79108-1_1. URL https://doi.org/10.1007/978-3-319-79108-1_1.
- [2] Christopher Alexander, Sara Ishikawa, and Murray Silverstein. *A Pattern Language: Towns, buildings, construction*, volume 2 of *Center for Environmental Structure Series*. Oxford University Press, New York, 1977.

[3] Mohammad Babaeizadeh, Chelsea Finn, Dumitru Erhan, Roy H. Campbell, and Sergey Levine. Stochastic Variational Video Prediction, March 2018. URL <https://doi.org/10.48550/arXiv.1710.11252>.

[4] John C. Baez and Jade Master. Open Petri Nets. *Mathematical Structures in Computer Science*, 30(3): 314–341, March 2020. ISSN 0960-1295, 1469-8072. doi: 10.1017/S0960129520000043. URL <http://arxiv.org/abs/1808.05415>.

[5] Francois Bancilhon and Nicolas Spyratos. Update semantics of relational views. *ACM Trans. Database Syst.*, 6(4):557–575, dec 1981. ISSN 0362-5915. doi: 10.1145/319628.319634. URL <https://doi.org/10.1145/319628.319634>.

[6] Kent Beck and Ward Cunningham. Using Pattern Languages for Object-Oriented Programs. Technical Report CR-87-43, September 1987.

[7] Samy Bengio, Oriol Vinyals, Navdeep Jaitly, and Noam Shazeer. Scheduled sampling for sequence prediction with recurrent neural networks. In C. Cortes, N. Lawrence, D. Lee, M. Sugiyama, and R. Garnett, editors, *Advances in Neural Information Processing Systems*, volume 28. Curran Associates, Inc., 2015. URL https://proceedings.neurips.cc/paper_files/paper/2015/file/e995f98d56967d946471af29d7bf99f1-Paper.pdf.

[8] Guillaume Boisseau and Paweł Sobociński. String Diagrammatic Electrical Circuit Theory. *Electronic Proceedings in Theoretical Computer Science*, 372:178–191, November 2022. ISSN 2075-2180. doi: 10.4204/EPTCS.372.13. URL <http://arxiv.org/abs/2106.07763>.

[9] Filippo Bonchi, Paweł Sobociński, and Fabio Zanasi. A Categorical Semantics of Signal Flow Graphs. In *CONCUR 2014 - Concurrency Theory - 25th International Conference*, Rome, Italy, September 2014. URL <https://hal.science/hal-02134182>.

[10] Filippo Bonchi, Paweł Sobociński, and Fabio Zanasi. Interacting Hopf Algebras. *Journal of Pure and Applied Algebra*, 221(1):144–184, January 2017. ISSN 00224049. doi: 10.1016/j.jpaa.2016.06.002. URL <http://arxiv.org/abs/1403.7048>.

[11] Filippo Bonchi, Robin Piedeleu, Paweł Sobociński, and Fabio Zanasi. Graphical Affine Algebra. In *2019 34th Annual ACM/IEEE Symposium on Logic in Computer Science (LICS)*, pages 1–12, June 2019. doi: 10.1109/LICS.2019.8785877. URL <https://doi.org/10.1109/LICS.2019.8785877>.

[12] Sam Bond-Taylor, Adam Leach, Yang Long, and Chris G. Willcocks. Deep Generative Modelling: A Comparative Review of VAEs, GANs, Normalizing Flows, Energy-Based and Autoregressive Models. *IEEE Transactions on Pattern Analysis and Machine Intelligence*, 44(11):7327–7347, November 2022. ISSN 0162-8828, 2160-9292, 1939-3539. doi: 10.1109/TPAMI.2021.3116668. URL <https://doi.org/10.48550/arXiv.2103.04922>.

[13] Samuel R. Bowman, Luke Vilnis, Oriol Vinyals, Andrew Dai, Rafal Jozefowicz, and Samy Bengio. Generating Sentences from a Continuous Space. In *Proceedings of The 20th SIGNLL Conference on Computational Natural Language Learning*, pages 10–21, Berlin, Germany, 2016. Association for Computational Linguistics. doi: 10.18653/v1/K16-1002. URL <https://doi.org/10.48550/arXiv.1511.06349>.

[14] Michael M. Bronstein, Joan Bruna, Taco Cohen, and Petar Veličković. Geometric Deep Learning: Grids, Groups, Graphs, Geodesics, and Gauges, May 2021. URL <https://doi.org/10.48550/arXiv.2104.13478>.

[15] Kenta Cho and Bart Jacobs. Disintegration and Bayesian Inversion via String Diagrams. *Mathematical Structures in Computer Science*, 29(7):938–971, August 2019. ISSN 0960-1295, 1469-8072. doi: 10.1017/S0960129518000488. URL <https://doi.org/10.48550/arXiv.1709.00322>.

[16] Casey Chu, Andrey Zhmoginov, and Mark Sandler. Cyclegan, a master of steganography. *arXiv preprint arXiv:1712.02950*, 2017. URL <https://doi.org/10.48550/arXiv.1712.02950>.

[17] Lorenzo Ciampiconi, Adam Elwood, Marco Leonardi, Ashraf Mohamed, and Alessandro Rozza. A survey and taxonomy of loss functions in machine learning, January 2023. URL <https://doi.org/10.48550/arXiv.2301.05579>.

[18] Bob Coecke and Ross Duncan. Interacting quantum observables: categorical algebra and diagrammatics. *New Journal of Physics*, 13(4):043016, April 2011. doi: 10.1088/1367-2630/13/4/043016. URL <https://dx.doi.org/10.1088/1367-2630/13/4/043016>.

[19] Bob Coecke and Aleks Kissinger. *Picturing Quantum Processes: A First Course in Quantum Theory and Diagrammatic Reasoning*. Cambridge University Press, Cambridge, 2017. ISBN 978-1-107-10422-8. doi: 10.1017/9781316219317. URL <https://www.cambridge.org/core/books/picturing-quantum-processes/1119568B3101F3A685BE832FEEC53E52>.

[20] Bob Coecke, Mehrnoosh Sadrzadeh, and Stephen Clark. Mathematical Foundations for a Compositional Distributional Model of Meaning, March 2010. URL <http://arxiv.org/abs/1003.4394>.

[21] Geoffrey SH Cruttwell, Bruno Gavranović, Neil Ghani, Paul Wilson, and Fabio Zanasi. Categorical foundations of gradient-based learning. In *Programming Languages and Systems: 31st European Symposium on Programming, ESOP 2022, Held as Part of the European Joint Conferences on Theory and Practice of Software, ETAPS 2022, Munich, Germany, April 2–7, 2022, Proceedings*, pages 1–28. Springer International Publishing Cham, 2022. URL <https://doi.org/10.48550/arXiv.2103.01931>.

[22] Artur d’Avila Garcez and Luis C. Lamb. Neurosymbolic AI: The 3rd Wave. <https://arxiv.org/abs/2012.05876v2>, December 2020.

[23] Gintare Karolina Dziugaite, Zoubin Ghahramani, and Daniel M. Roy. A study of the effect of JPG compression on adversarial images, August 2016. URL <https://doi.org/10.48550/arXiv.1608.00853>.

[24] Brendan Fong and David I. Spivak. *An Invitation to Applied Category Theory: Seven Sketches in Compositionality*. Cambridge University Press, 1 edition, July 2019. ISBN 978-1-108-66880-4 978-1-108-48229-5 978-1-108-71182-1. doi: 10.1017/9781108668804.

[25] Brendan Fong and David I. Spivak. Supplying bells and whistles in symmetric monoidal categories., August 2019. URL <https://doi.org/10.48550/arXiv.1908.02633>.

[26] Thomas Fox. Coalgebras and cartesian categories. *Communications in Algebra*, 4(7):665–667, January 1976. ISSN 0092-7872. doi: 10.1080/00927877608822127.

[27] Thomas Fox. Coalgebras and cartesian categories. *Communications in Algebra*, 4(7):665–667, January 1976. ISSN 0092-7872, 1532-4125. doi: 10.1080/00927877608822127. URL <https://doi.org/10.1080/00927877608822127>.

[28] Tobias Fritz. A synthetic approach to Markov kernels, conditional independence and theorems on sufficient statistics. *Advances in Mathematics*, 370:107239, August 2020. ISSN 00018708. doi: 10.1016/j.aim.2020.107239. URL <https://doi.org/10.1016/j.aim.2020.107239>.

[29] Tobias Fritz, Tomáš Gonda, and Paolo Perrone. De Finetti’s Theorem in Categorical Probability. *Journal of Stochastic Analysis*, 2(4), November 2021. ISSN 2689-6931. doi: 10.31390/josa.2.4.06. URL <http://arxiv.org/abs/2105.02639>.

[30] Huan Fu, Mingming Gong, Chaohui Wang, Kayhan Batmanghelich, Kun Zhang, and Dacheng Tao. Geometry-consistent generative adversarial networks for one-sided unsupervised domain mapping. In *Proceedings of the IEEE/CVF Conference on Computer Vision and Pattern Recognition (CVPR)*, June 2019.

[31] Bruno Gavranović, Paul Lessard, Andrew Dudzik, Tamara von Glehn, João G. M. Araújo, and Petar Veličković. Categorical deep learning: An algebraic theory of architectures, February 2024. URL <https://doi.org/10.48550/arXiv.2402.15332>.

[32] Ian Goodfellow, Jean Pouget-Abadie, Mehdi Mirza, Bing Xu, David Warde-Farley, Sherjil Ozair, Aaron Courville, and Yoshua Bengio. Generative adversarial networks. *Communications of the ACM*, 63(11):139–144, 2020. URL <https://doi.org/10.1145/3422622>.

[33] Nathan Haydon and Paweł Sobociński. Compositional Diagrammatic First-Order Logic. In Ahti-Veikko Pietarinen, Peter Chapman, Leonie Bosveld-de Smet, Valeria Giardino, James Coker, and Sven Linker, editors, *Diagrammatic Representation and Inference*, Lecture Notes in Computer Science, pages 402–418, Cham, 2020. Springer International Publishing. ISBN 978-3-030-54249-8. doi: 10.1007/978-3-030-54249-8_32. URL https://doi.org/10.1007/978-3-030-54249-8_32.

[34] Jules Hedges. String diagrams for game theory, March 2015. URL <http://arxiv.org/abs/1503.06072>.

[35] Amir Hertz, Ron Mokady, Jay Tenenbaum, Kfir Aberman, Yael Pritch, and Daniel Cohen-or. Prompt-to-prompt image editing with cross-attention control. In *The Eleventh International Conference on Learning Representations*, 2022. URL <https://doi.org/10.48550/arXiv.2208.01626>.

[36] Martin Hofmann, Benjamin Pierce, and Daniel Wagner. Symmetric lenses. *ACM SIGPLAN Notices*, 46(1):371–384, 2011.

[37] Kurt Hornik, Maxwell Stinchcombe, and Halbert White. Multilayer feedforward networks are universal approximators. *Neural networks*, 2(5):359–366, 1989.

[38] Bart Jacobs, Aleks Kissinger, and Fabio Zanasi. Causal inference by string diagram surgery. In *Foundations of Software Science and Computation Structures: 22nd International Conference, FOSSACS 2019, Held as Part of the European Joint Conferences on Theory and Practice of Software, ETAPS 2019, Prague, Czech Republic, April 6–11, 2019, Proceedings 22*, pages 313–329. Springer, 2019. URL https://doi.org/10.1007/978-3-030-17127-8_18.

[39] Bahjat Kawar, Shiran Zada, Oran Lang, Omer Tov, Huiwen Chang, Tali Dekel, Inbar Mosseri, and Michal Irani. Imagic: Text-based real image editing with diffusion models. In *Proceedings of the IEEE/CVF Conference on Computer Vision and Pattern Recognition (CVPR)*, pages 6007–6017, June 2023.

[40] Nikhil Khatri, Tuomas Laakkonen, Jonathon Liu, and Vincent Wang-Maścianica. On the anatomy of attention, 2024.

[41] Diederik P. Kingma and Max Welling. Auto-Encoding Variational Bayes, December 2022. URL <https://doi.org/10.48550/arXiv.1312.6114>.

[42] Jeremias Knoblauch, Jack Jewson, and Theodoros Damoulas. An Optimization-centric View on Bayes’ Rule: Reviewing and Generalizing Variational Inference. *Journal of Machine Learning Research*, 23:1–109, 2022.

[43] Juncen Li, Robin Jia, He He, and Percy Liang. Delete, retrieve, generate: a simple approach to sentiment and style transfer. In *Proceedings of the 2018 Conference of the North American Chapter of the Association for Computational Linguistics: Human Language Technologies, Volume 1 (Long Papers)*, pages 1865–1874, 2018. URL <https://doi.org/10.18653/v1/N18-1169>.

[44] Ziwei Liu, Ping Luo, Xiaogang Wang, and Xiaoou Tang. Deep learning face attributes in the wild. In *Proceedings of International Conference on Computer Vision (ICCV)*, December 2015.

[45] Robin Lorenz and Sean Tull. Causal models in string diagrams, April 2023. URL <https://doi.org/10.48550/arXiv.2304.07638>.

[46] Martin Markl, Steve Shnider, and Jim Stasheff. *Operads in Algebra, Topology and Physics*. American Mathematical Society, Providence, RI, July 2007. ISBN 978-0-8218-4362-8.

[47] Samuel G. Müller and Frank Hutter. Trivialaugment: Tuning-free yet state-of-the-art data augmentation, 2021.

[48] Keisuke Nakano. A Tangled Web of 12 Lens Laws. In *Reversible Computation: 13th International Conference, RC 2021, Virtual Event, July 7–8, 2021, Proceedings*, pages 185–203, Berlin, Heidelberg, July 2021. Springer-Verlag. ISBN 978-3-030-79836-9. doi: 10.1007/978-3-030-79837-6_11.

[49] Andrew Ng and Michael Jordan. On Discriminative vs. Generative Classifiers: A comparison of logistic regression and naive Bayes. In *Advances in Neural Information Processing Systems*, volume 14. MIT Press, 2001.

[50] nLab authors. Bayesian inversion. <https://ncatlab.org/nlab/show/Bayesian+inversion>, June 2024. Revision 9.

[51] nLab authors. Markov category. <https://ncatlab.org/nlab/show/Markov+category>, July 2024. Revision 56.

[52] Prakash Panangaden. The Category of Markov Kernels. *Electr. Notes Theor. Comput. Sci.*, 22:171–187, December 1999. doi: 10.1016/S1571-0661(05)80602-4. URL [https://doi.org/10.1016/S1571-0661\(05\)80602-4](https://doi.org/10.1016/S1571-0661(05)80602-4).

[53] Dusko Pavlovic. Monoidal computer i: Basic computability by string diagrams. *Information and Computation*, 226:94–116, 2013. ISSN 0890-5401. doi: <https://doi.org/10.1016/j.ic.2013.03.007>. URL <https://www.sciencedirect.com/science/article/pii/S0890540113000254>. Special Issue: Information Security as a Resource.

[54] Dusko Pavlovic. *Programs as Diagrams: From Categorical Computability to Computable Categories*. Springer, 1st ed. 2023 edition edition, September 2023. ISBN 978-3-031-34826-6. URL <https://doi.org/10.48550/arXiv.2208.03817>.

[55] Boldizsár Poór, Quanlong Wang, Razin A. Shaikh, Lia Yeh, Richie Yeung, and Bob Coecke. Completeness for arbitrary finite dimensions of ZXW-calculus, a unifying calculus, April 2023. URL <http://arxiv.org/abs/2302.12135>.

[56] Alec Radford and Karthik Narasimhan. Improving language understanding by generative pre-training. 2018. URL <https://api.semanticscholar.org/CorpusID:49313245>.

[57] Marc'Aurelio Ranzato, Y-Lan Boureau, Sumit Chopra, and Yann LeCun. A unified energy-based framework for unsupervised learning. In Marina Meila and Xiaotong Shen, editors, *Proceedings of the Eleventh International Conference on Artificial Intelligence and Statistics*, volume 2 of *Proceedings of Machine Learning Research*, pages 371–379, San Juan, Puerto Rico, 21–24 Mar 2007. PMLR. URL <https://proceedings.mlr.press/v2/ranzato07a.html>.

[58] Oliver E. Richardson. Loss as the inconsistency of a probabilistic dependency graph: Choose your model, not your loss function. In Gustau Camps-Valls, Francisco J. R. Ruiz, and Isabel Valera, editors, *Proceedings of The 25th International Conference on Artificial Intelligence and Statistics*, volume 151 of *Proceedings of Machine Learning Research*, pages 2706–2735. PMLR, 28–30 Mar 2022. URL <https://proceedings.mlr.press/v151/richardson22b.html>.

[59] Joseph Rocca. Understanding Variational Autoencoders (VAEs). <https://towardsdatascience.com/understanding-variational-autoencoders-vae-f70510919f73>, March 2021.

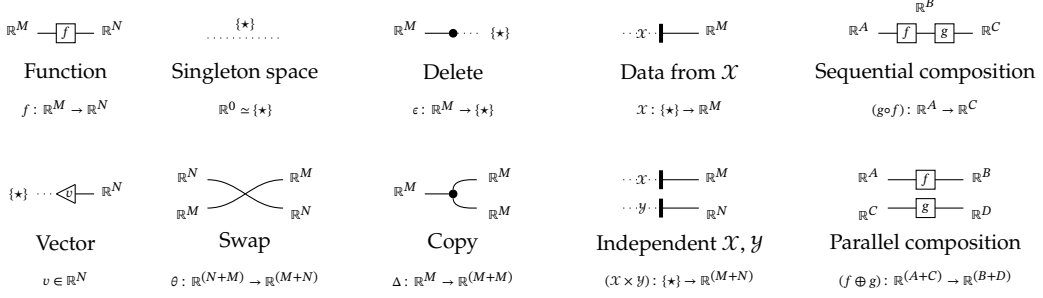
[60] Peter Selinger. A Survey of Graphical Languages for Monoidal Categories. In Bob Coecke, editor, *New Structures for Physics*, pages 289–355. Springer Berlin Heidelberg, Berlin, Heidelberg, 2011. ISBN 978-3-642-12821-9. doi: 10.1007/978-3-642-12821-9_4. URL https://doi.org/10.1007/978-3-642-12821-9_4.

[61] Lennert De Smet, Pedro Zuidberg Dos Martires, Robin Manhaeve, Giuseppe Marra, Angelika Kimmig, and Luc De Raedt. Neural probabilistic logic programming in discrete-continuous domains. In *Proceedings of the Thirty-Ninth Conference on Uncertainty in Artificial Intelligence*, pages 529–538. PMLR, July 2023.

- [62] Paweł Sobociński. Graphical Linear Algebra, June 2015. URL <https://graphicallinearalgebra.net/>.
- [63] Akhilesh Sudhakar, Bhargav Upadhyay, and Arjun Maheswaran. “Transforming” delete, retrieve, generate approach for controlled text style transfer. In *Proceedings of the 2019 Conference on Empirical Methods in Natural Language Processing and the 9th International Joint Conference on Natural Language Processing (EMNLP-IJCNLP)*, pages 3269–3279, 2019. URL <https://doi.org/10.48550/arXiv.1908.09368>.
- [64] Richard Sutton. The Bitter Lesson, 2019.
- [65] Juan Terven, Diana M. Cordova-Esparza, Alfonso Ramirez-Pedraza, and Edgar A. Chavez-Urbiola. Loss Functions and Metrics in Deep Learning, September 2023. URL <https://doi.org/10.48550/arXiv.2307.0269>.
- [66] Vladimir N. Vapnik. *Statistical Learning Theory*. Wiley-Interscience, New York, 1st edition edition, September 1998. ISBN 978-0-471-03003-4.
- [67] V. Wang-Maścianica. *String Diagrams for Text*. <http://purl.org/dc/dcmitype/Text>, University of Oxford, 2023.
- [68] Vincent Wang-Mascianica, Jonathon Liu, and Bob Coecke. Distilling Text into Circuits, January 2023. URL <http://arxiv.org/abs/2301.10595>.
- [69] Nicholas Watters, Loic Matthey, Sebastian Borgeaud, Rishabh Kabra, and Alexander Lerchner. Spriteworld: A flexible, configurable reinforcement learning environment, 2019. URL <https://github.com/deepmind/spriteworld/>.
- [70] Ronald J. Williams and David Zipser. A learning algorithm for continually running fully recurrent neural networks. *Neural Computation*, 1(2):270–280, 1989. doi: 10.1162/neco.1989.1.2.270. URL <https://doi.org/10.1162/neco.1989.1.2.270>.
- [71] Sidi Wu, Yizi Chen, Samuel Mermet, Lorenz Hurni, Konrad Schindler, Nicolas Gonthier, and Loic Landrieu. Stegogan: Leveraging steganography for non-bijective image-to-image translation, March 2024. URL <https://doi.org/10.48550/arXiv.2403.20142>.
- [72] Donald Yau. Higher dimensional algebras via colored PROPs, September 2008. URL <https://doi.org/10.48550/arXiv.0809.2161>.
- [73] Jun-Yan Zhu, Taesung Park, Phillip Isola, and Alexei A Efros. Unpaired image-to-image translation using cycle-consistent adversarial networks, 2017.

A String diagrams for tasks

String diagrams are a formal diagrammatic syntax that take semantics in symmetric monoidal categories, and they find usage in a broad variety of fields⁴. Our string diagrams are built using sequential and parallel composition from the following generators, along with a stock of function labels:



For conventional reasons that were not by our choice, vectors are depicted as triangular nodes with only output wires, reminiscent of bra-ket notation. (co)associative (co)monoids, such as copy-delete and add-zero, are specially depicted as circular nodes as is common in applied category theory. In this work, encoders and decoders are sometimes depicted as "bottlenecking" trapezia, as is common in ML, and distributional states are given their own notation as thick bars.

An attractive characteristic of string diagrams is that visually intuitive equivalences between information flows are guaranteed to correspond to symbolic derivations of behavioural equivalence: tedious algebraic proofs of equality between sequentially- and parallel-composite processes are suppressed and absorbed by (processive) isotopies of diagrams. In the diagrammatic syntax it is conventional to notate such isomorphisms as plain equalities. Interested readers are referred to [60] for the relevant mathematical foundations.

$$\begin{aligned}
 & (\mathbf{1} \oplus \theta) \circ (\Delta \oplus g) \circ (f \oplus \mathbf{1}) \\
 & \simeq (\mathbf{1} \oplus \theta) \circ (\mathbf{1} \oplus \mathbf{1} \oplus g) \circ (\Delta \oplus \mathbf{1}) \circ (f \oplus \mathbf{1}) & [\text{Identity, interchange}] \\
 & \simeq (\mathbf{1} \oplus g \oplus \mathbf{1}) \circ (\mathbf{1} \oplus \theta) \circ (\Delta \oplus \mathbf{1}) \circ (f \oplus \mathbf{1}) & [\text{Braid naturality}] \\
 & \simeq (\mathbf{1} \oplus g \oplus \mathbf{1}) \circ (\mathbf{1} \oplus \theta) \circ (f \oplus f \oplus \mathbf{1}) \circ (\Delta \oplus \mathbf{1}) & [\text{Copy naturality}] \\
 & \simeq (\mathbf{1} \oplus g \oplus \mathbf{1}) \circ (f \oplus \mathbf{1} \oplus f) \circ (\mathbf{1} \oplus \theta) \circ (\Delta \oplus \mathbf{1}) & [\text{Braid naturality}]
 \end{aligned}
 \Leftrightarrow
 \begin{array}{c}
 \text{Diagram showing two isotopic configurations of a string diagram involving } f, g, \Delta, \theta, \text{ and } \mathbf{1} \text{ nodes.}
 \end{array}$$

A.1 Categorical semantics of task diagrams

The functional effect of the construction below is to extend the category of continuous maps between Euclidean spaces with global elements that behave as probability distributions instead of points. We presume familiarity with symmetric monoidal categories and their graphical calculi [60].

Let **CartSp** denote the coloured PROP [72] of continuous maps between Euclidean spaces, where the tensor product is the cartesian product — i.e. **CartSp** is cartesian monoidal.

Let **BorelStoch** denote the Markov category [15, 28] of stochastic kernels [52] between Borel-measurable spaces. Stochastic kernels in particular subsume the continuous maps between Euclidean spaces.

As a Markov category, in the terminology of [25], **BorelStoch** supplies cocommutative comonoids. By Fox's theorem [27] cartesian monoidal categories are precisely those isomorphic to their own categories of cocommutative comonoids. Hence there is a (semicartesian) functorial embedding of **CartSp** into **BorelStoch** sending \mathbb{R}^N to \mathbb{R}^N (equipped with the usual Borel measure), and continuous maps to deterministic continuous maps. We declare our semantics to be taken in the category to be generated by the image of this embedding along with the probability distributions $\mathcal{X} : \{\star\} \rightarrow \mathbb{R}^N$, where $\{\star\}$ is the singleton monoidal unit of **BorelStoch**.

⁴Including linear and affine algebra [62, 10, 11], first order logic [33], causal models [45, 38], signal flow graphs [9], electrical circuits [8], game theory [34], petri nets [4], probability theory [29], formal linguistics [20, 68, 67], quantum theory [18, 19, 55], and aspects of machine learning such as backpropagation [21].

A.2 Categorical semantics for idealised universal approximators

As we are concerned with behaviour, not implementation details, we idealise all neural networks as perfect universal approximators, which we may formulate string-diagrammatically in a monoidal closed category, borrowing evaluator-notation from [53, 54]. In essence, we are assuming that architectures are sufficiently expressive to optimise whatever tasks we give them; in practice, the conditions under which architectures become universal approximators can be mild [37], and the idealisation is increasingly true-in-practice in the contemporary context of increasing data and compute.

Definition A.1 (Learner). Let X, Y denote input and output types. A process $\Omega : \mathbf{p} \oplus X \rightarrow Y$ with parameters in $\text{para}(\Omega) = \mathbf{p} = \mathbb{R}^n$ (for sufficiently large n) is a *universal approximator* or *learner* when⁵:

$$\forall f_{X \rightarrow Y} \exists \hat{f}_{\mathbf{p}} : \quad \boxed{f} \quad = \quad \boxed{\Omega} \quad \text{with } \mathbf{p} \text{ label}$$

The parameter space could represent e.g. the phase space of weights and biases of a neural network.

Example A.2. By visual convention, we use colours to indicate different data types of wires. We depict processes with no free parameters as white boxes, and learners as black-boxes with variable labels to indicate distinct or shared parameters. The following composite process has one function f with no learnable parameters, and three neural nets: the two labelled α share a parameter in the space \mathbf{p} , and the one labelled β takes a parameter in \mathbf{Q} . In this paper, we favour the shorthand on the right.

$$\begin{array}{c} \text{Diagram showing a composite process with two learners } \alpha \text{ sharing a parameter in } \mathbf{p}, \text{ and one learner } \beta \text{ taking a parameter in } \mathbf{Q}. \end{array}$$

The universal approximation theorem, suitably idealised, manifests as the capacity for a black-box learner to be diagrammatically substituted for any other composite diagram with equal input and output, including those composites that contain other learners. For example, recall the linear put below, which may be viewed as substituting a particular composite of put', enc, dec, and addition in place of put:

$$\begin{array}{c} \text{Diagram showing the equivalence between a simple put box and a more complex composite involving enc, dec, and addition.} \end{array}$$

This ability is referred to in this work intermittently as *specialisation*, and as *expressive reduction* in [40] where the concept first appeared. For the sake of completeness, we reproduce the relevant construction that gives category-theoretic semantics to universal approximators and specialisation below, along with standard definitions, with the authors' permission.

Definition A.3 (PROP). A PROP is a strict symmetric monoidal category generated by a single object x : every object is of the form

$$\bigotimes^n x = x \underbrace{\otimes \cdots \otimes x}_n$$

PROPs may be generated by, and presented as *signatures* (Σ, E) consisting of generating morphisms Σ with arity and coarity in \mathbb{N} , and equations E relating symmetric monoidal composites of generators.

Definition A.4 (Coloured PROP). A *multi-sorted* or *coloured* PROP with set of colours \mathfrak{C} has a monoid of objects generated by \mathfrak{C} .

Definition A.5 (Cartesian PROP). By Fox's theorem [26], a cartesian PROP is one in which every object (wire) is equipped with a cocommutative comonoid (copy) with counit (delete) such that all morphisms in the category are comonoid cohomomorphisms.

⁵We adapt the shape of the universal approximators to clearly indicate the parameters.

Definition A.6 ((symmetric, unital) coloured operad). Where $(\mathcal{V}, \boxtimes, J)$ is a symmetric monoidal category and \mathfrak{C} denotes a set of colours c_i , a coloured operad \mathcal{O} consists of:

- For each $n \in \mathbb{N}$ and each $(n + 1)$ -tuple $(c_1, \dots, c_n; c)$, an object $\mathcal{O}(c_1, \dots, c_n; n) \in \mathcal{V}$
- For each $c \in \mathfrak{C}$, a morphism $1_c : J \rightarrow \mathcal{O}(c; c)$ called the *identity of c*
- For each $(n + 1)$ -tuple $(c_1 \dots c_n; c)$ and n other tuples $(d_1^1 \dots d_{k_1}^1) \dots (d_1^n \dots d_{k_n}^n)$ a *composition morphism*

$$\mathcal{O}(c_1, \dots, c_n; c) \boxtimes \mathcal{O}(d_1^1 \dots d_{k_1}^1) \boxtimes \dots \boxtimes \mathcal{O}(d_1^n \dots d_{k_n}^n) \rightarrow \mathcal{O}(d_1^1 \dots d_{k_1}^1 \dots d_1^n \dots d_{k_n}^n; c)$$

- for all $n \in \mathbb{N}$, all tuples of colours, and each permutation $\sigma \in S_n$ the symmetric group on n , a morphism:

$$\sigma^* : \mathcal{O}(c_1 \dots c_n; c) \rightarrow \mathcal{O}(c_{\sigma^*(1)} \dots c_{\sigma^*(n)}; c)$$

The σ^* must represent S_n , and composition must satisfy associativity and unitality in a S_n -invariant manner.

Construction A.7 (Hom-Operad of coloured PROP). Where $(\mathcal{P}, \otimes, I)$ is a coloured PROP with colours $\mathfrak{C}_{\mathcal{P}}$, we construct $\mathcal{O}_{\mathcal{P}}$, the *hom-operad* of \mathcal{P} . We do so in two stages, by first defining an ambient operad, and then restricting to the operad obtained by a collection of generators. Let the ambient symmetric monoidal category be $(\mathbf{Set}, \times, \{\star\})$. Let the colours $\mathfrak{C}_{\mathcal{O}}$ be the set of all tuples (\mathbf{A}, \mathbf{B}) , each denoting a pair of tuples $(A_1 \otimes A_n, B_1 \otimes B_n)$ of $A_i, B_i \in \mathfrak{C}_{\mathcal{P}}$.

- The tuple $((\mathbf{A}^1, \mathbf{B}^1) \dots (\mathbf{A}^n, \mathbf{B}^n); (\mathbf{A}, \mathbf{B}))$ is assigned the set $[\mathcal{P}(\mathbf{A}^1, \mathbf{B}^1) \times \dots \times \mathcal{P}(\mathbf{A}^n, \mathbf{B}^n) \rightarrow \mathcal{P}(\mathbf{A}, \mathbf{B})] \in \mathbf{Set}$; the set of all *generated* functions from the product of homsets $\mathcal{P}(\mathbf{A}^i, \mathbf{B}^i)$ to the homset $\mathcal{P}(\mathbf{A}, \mathbf{B})$.
- $1_{(\mathbf{A}, \mathbf{B})} : \{\star\} \rightarrow [\mathcal{P}(\mathbf{A}, \mathbf{B}) \rightarrow \mathcal{P}(\mathbf{A}, \mathbf{B})]$ is the identity functional that maps $f : \mathbf{A} \rightarrow \mathbf{B}$ in $\mathcal{P}(\mathbf{A}, \mathbf{B})$ to itself.
- The composition operations correspond to function composition in \mathbf{Set} , where $[X \rightarrow Y] \times [Y \rightarrow Z] \rightarrow [X \rightarrow Z]$ sends $(f : X \rightarrow Y, g : Y \rightarrow Z) \mapsto (g \circ f) : X \rightarrow Z$; appropriately generalised to the multi-argument case. The permutations are similarly defined, inheriting their coherence conditions from the commutativity isomorphisms of the categorical product \times .

The generators are:

- For every $f \in \mathcal{P}(\mathbf{A}, \mathbf{B})$ that is a generator of \mathcal{P} , define a corresponding generator of type $\{\star\} \rightarrow [\mathcal{P}(I, I) \rightarrow \mathcal{P}(\mathbf{A}, \mathbf{B})]$, which is the functional $(- \mapsto (f \otimes -))$ that sends endomorphisms of the monoidal unit of \mathcal{P} to their tensor with f , viewed as an element of the set $[\mathcal{P}(I, I) \rightarrow \mathcal{P}(\mathbf{A}, \mathbf{B})]$.
- For every pair of tuples $((\mathbf{X}^1, \mathbf{Y}^1) \dots (\mathbf{X}^m, \mathbf{Y}^m); (\mathbf{A}, \mathbf{B}))$ and $((\mathbf{J}^1, \mathbf{K}^1) \dots (\mathbf{J}^n, \mathbf{K}^n); (\mathbf{B}, \mathbf{C}))$ in $\mathfrak{C}_{\mathcal{O}}$, a corresponding *sequential composition* operation of type:

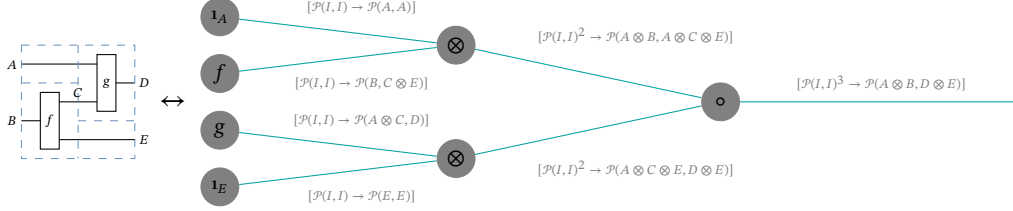
$$\begin{aligned} & [\prod_{i \leq m} \mathcal{P}(\mathbf{X}^i, \mathbf{Y}^i) \rightarrow \mathcal{P}(\mathbf{A}, \mathbf{B})] \times [\prod_{j \leq n} \mathcal{P}(\mathbf{J}^j, \mathbf{K}^j) \rightarrow \mathcal{P}(\mathbf{B}, \mathbf{C})] \\ & \rightarrow [(\prod_{i \leq m} \mathcal{P}(\mathbf{X}^i, \mathbf{Y}^i) \times \prod_{j \leq n} \mathcal{P}(\mathbf{J}^j, \mathbf{K}^j)) \rightarrow \mathcal{P}(\mathbf{A}, \mathbf{C})] \end{aligned}$$

Which maps pairs of functionals $(F : \prod_{i \leq m} \mathcal{P}(\mathbf{X}^i, \mathbf{Y}^i) \rightarrow \mathcal{P}(\mathbf{A}, \mathbf{B}), G : \prod_{j \leq n} \mathcal{P}(\mathbf{J}^j, \mathbf{K}^j) \rightarrow \mathcal{P}(\mathbf{B}, \mathbf{C}))$ to the functional which sends $p^i : \mathbf{X}^i \rightarrow \mathbf{Y}^i$ and $q^j : \mathbf{J}^j \rightarrow \mathbf{K}^j$ to $G(p_1 \dots p_m) \circ F(q_1 \dots q_n)$.

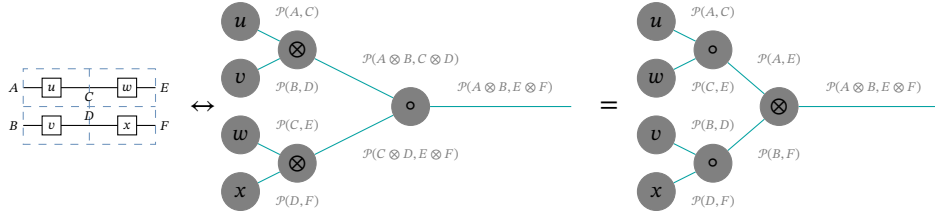
- An analogous *parallel composition* for every pair of tuples, which sends pairs of functionals (F, G) to $G(p_1 \dots p_m) \otimes F(q_1 \dots q_n)$.

Remark A.8. For technical reasons involving scalars (the endomorphisms of the monoidal unit), this construction only works in semicartesian settings, i.e. where the monoidal unit is also terminal, but that is sufficiently general to admit our use cases, which are primarily in cartesian monoidal settings [26] and semicartesian Markov categories for probabilistic settings [51].

Example A.9. Construction A.7 can be thought of as bridging diagrams with their specific algebraic descriptions using just the basic constructors \circ, \otimes ; the hom-operad (when notated suggestively in the usual tree-notation, found e.g. in [46]) plays the role of the syntactic tree of \circ, \otimes operators. For instance, given the composite morphism $(g \otimes 1_E) \circ (1_A \otimes f)$ in PROP \mathcal{P} , the corresponding diagram and operad-state in $\mathcal{O}_{\mathcal{P}}$ is:

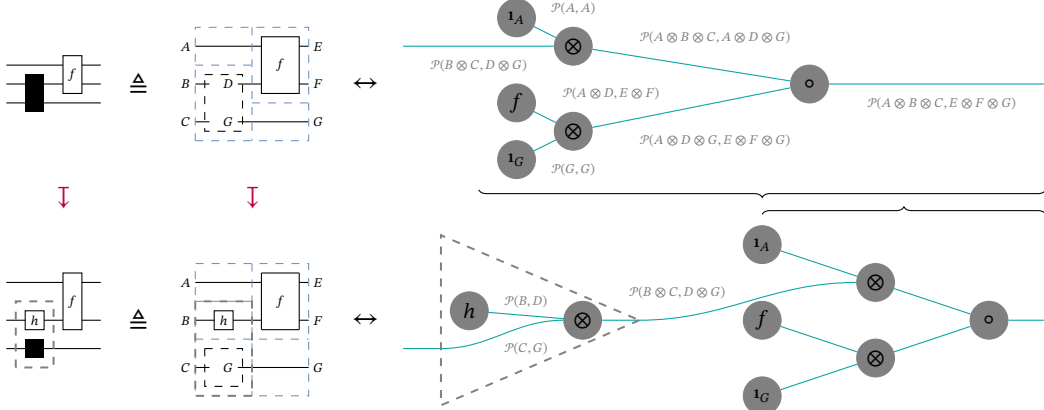


Since the PROPs **CartSp** and its free tensoring are cartesian, $\mathcal{P}(I, I)$ is a singleton containing only the identity of the monoidal unit, so in the settings we are concerned with, we may simplify colours of the form $[\mathcal{P}(I, I)^N \rightarrow \mathcal{P}(\mathbf{A}, \mathbf{B})]$ to just $\mathcal{P}(\mathbf{A}, \mathbf{B})$, and operad-states $\{\star\} \rightarrow \mathcal{P}(\mathbf{A}, \mathbf{B})$ are in bijective correspondence with morphisms $f : \mathbf{A} \rightarrow \mathbf{B}$ of \mathcal{P} ; the fact that all $f : \mathbf{A} \rightarrow \mathbf{B}$ are representable as operad states follows by construction, since any f in \mathcal{P} is by definition expressible in terms of the generators of \mathcal{P} , and sequential and parallel composition \circ, \otimes . As we assume homsets are already quotiented by the equational theory of \mathcal{P} and the symmetric monoidal coherences, our operadic representations inherit them: for example, we obtain interchange equalities such as the one below for free:



Definition A.10 (Universal approximators and specialisation). A morphism of a coloured PROP \mathcal{P} of type (\mathbf{A}, \mathbf{B}) containing universal approximators as black-boxes of types $\mathbf{A}^{i \leq n} \rightarrow \mathbf{B}^{i \leq n}$ is a morphism $((\mathbf{A}^1, \mathbf{B}^1) \cdots (\mathbf{A}^n, \mathbf{B}^n); (\mathbf{A}, \mathbf{B}))$ of $\mathcal{O}_{\mathcal{P}}$, and by construction, vice versa. Specialisation corresponds to pre-composition in $\mathcal{O}_{\mathcal{P}}$.

Example A.11. The inputs of open morphisms in $\mathcal{O}_{\mathcal{P}}$ correspond to "typed holes", and operadic precomposition corresponds to "filling holes", with contents that may themselves also contain typed holes. This precisely formalises the intuition that expressive reductions correspond to the ability of a universal approximator to simulate anything, including composites containing other universal approximators.



Remark A.12. The extension of the current theory to accommodate parameter sharing between universal approximators is conceptually straightforward but technically involved. Parameter sharing corresponds to the ability to reuse – i.e. copy – data between open wires in the operad $\mathcal{O}_{\mathcal{P}}$, which amounts to having a cartesian operad.

B Strong manipulation

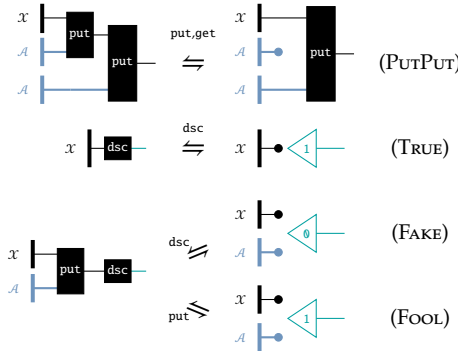
The basic manipulation admits pathological counterexamples, which we may block by imposing additional tasks. We can treat these new tasks as additional regularisation terms. This section further illustrates a form of "legalistic" thinking using tasks: by thinking of ways that "noncooperative" or "naughty" learners might seek to satisfy tasks without exhibiting the behaviour that the modeller desires. By identifying these counterexamples and constructing additional tasks that block them, the modeller may iteratively improve the behaviour of the model. For illustration, consider the following examples of pathological behaviour that satisfy basic manipulation, again in the setting of editing the colour of a shape.

Example B.1 (Flipping). Consider a put that changes the colour of a shape as desired, but then vertically flips the shape. If the classifier get is insensitive to the position and orientation of the shape, then CLASSIFY, PUTGET, and GETPUT are satisfied. Moreover, since a vertical flip is its own inverse, composing two puts as in the UNDOABILITY task will not detect this aberration. Speaking in more general terms, if there are properties that get is insensitive to, there must be additional guardrails to ensure that put preserves these other properties as the identity, rather than one of potentially very many self-inverse symmetries.

Example B.2 (Adversarial decorations). While the classifier get may be perfect in-distribution, there are no guarantees about its behaviour out of distribution, for example, when given images with multiple shapes, where it might only classify the leftmost shape. So, it is possible that put learns to make edits that take the resulting image out-of-distribution: for example, by adding a red circle next to a blue square to fool the classifier into outputting "red". This would satisfy CLASSIFY, PUTGET, and GETPUT. If the put can recognise and undo its own decorations, then UNDOABILITY will also be satisfied. Speaking more generally, we require additional guardrails to ensure that put returns something in-distribution.

The strong manipulation adds additional tasks to the manipulator. A strong manipulator has to satisfy the original four tasks plus the following four:

Task B.3 (strong manipulation add-ons).



The PutPut task (which is strictly stronger than UNDOABILITY in that it is algebraically implied) says that the effect of putting twice is the same as discarding the effect of the first edit and only keeping the last edit. In conjunction with PUTGET and GETPUT, this creates what is known in the literature as a *very well-behaved lens*, which blocks Example B.1 and similar modifications of the data get is insensitive to.

The TRUE, FAKE, and FOOL tasks introduce a discriminator component dsc, which forms a GAN pattern with respect to put as the generator. When well-trained, this forces the outputs of put to lie in-distribution. As in general there are no algebraic or equational laws that characterise arbitrary distributions of data, using GANs in this way is a generic recipe for shaping outputs of generators to behave well in-distribution.

Remark B.4 (Why basic manipulation is preferable in practice). We have observed informally that conditions such as those in basic manipulation where learners are cooperative and there are only learners on the LHS appear to be more stable during training. We suggest a sketch reason why: in the tasks of strong manipulation, PutPut has put occur on both the LHS and RHS, which establishes a nontrivial dependence on the current position on parameter-space of put in the process of finding a solution. Similarly, the GAN rules of strong manipulation establishes adversarial mutual dependencies in the parameters of dsc and put. Conceptually, these dependencies create dynamical systems on the paths that the learners take over the course of training in parameter-space, which may for instance include stable orbits and chaotic behaviour, and may be highly sensitive to initial conditions. A further elaboration of "static" versus "dynamic" tasks in tandem with the ability to express equivalent tasks is potentially useful for creating train-stable models with equivalent behaviour, but this is beyond the scope of this paper, and left for future work.

C Experiment Details

C.1 Spriteworld

For the Spriteworld experiment, we procedurally generate 32x32 images containing a single shape with the following attributes:

Attributes	Possible Values
Shape	{ Ellipse, Rectangle, Triangle }
Hue	{ Red : 0 ± 8 , Green : 85 ± 8 , Blue : 170 ± 8 }
Saturation	64-255
Value	64-255
Background Color	Black
Width & Height	5-27
X & Y position	5-27

Only the first two attributes, shape and hue, are changed in the `manipulation` task, but all unchanged properties are intended to be preserved by the transformation. We use an autoencoder with a CNN/DCNN architecture to embed each image into a latent space:

Parameter	Value
Latent Size	32
Layers	4
Hidden Channels	64
Kernel Size	5x5
Stride	2
Activation Function	LeakyReLU(0.1) followed by BatchNorm

We train separate `get`/`put` models for each of the three concepts: shape, colour, blue-circleness. Each model uses the encoder of the autoencoder to embed input images into latent space, and only sees the labels for the particular attribute it is manipulating.

For shape and colour, the `get` model uses a linear classifier from the latent space (of size 32) to 3 output logit values, one for each possible value. The `put` model maps a one-hot vector of the input value to a vector in latent space that is added to the embedding. This new embedding is then decoded by the autoencoder.

For blue-circleness, the `get` model uses a linear classifier from the latent space to a single output value from zero to one (we do not use a sigmoid output layer to restrict the output). The `put` model uses a complement of size 8. It concatenates the one-hot value vector with the image embedding and the complement vector (using a default trainable complement vector if one is not provided) and passes that through a linear layer to get a new embedding vector (which is then decoded) and complement vector.

In total, these models contain 644,130 parameters. All models are trained simultaneously according to the `autoencoding` and `manipulation` rules, along with `PUTPUT`. At each step, a batch of images is generated, along with four batches of random values, containing random labels for the shape and colour manipulators, and random real numbers for the blue-circleness manipulator, uniformly sampled from $[-0.1, 1.1]$ and then clamped to $[0, 1]$. The loss function is a weighted sum of the losses from each atomic task in order to balance the signal from the image loss with the signal from the classifier loss:

Hyper-parameter	Value	Task	Weight
Steps	100,000	AUTOENCODING	100
Batch Size	512	GETPUT	1
Optimiser	AdamW	PUTPUT	1
Learning Rate	10^{-3}	UNDO	10
Weight Decay	10^{-2}	PUTGET	
Gradient Clipping	1 (element-wise)	(blue-circleness)	10
Image Loss	$L_2 + 0.25 \cdot L_1$	(shape and colour)	1
Discrete Value Loss	Binary cross-entropy	CLASSIFICATION	
Continuous Value Loss	Mean squared error	(blue-circleness)	10
Seed	0	(shape and colour)	1

C.2 Faces

For the faces experiment, we use the *CelebFaces Attributes* dataset [44], with an off-the-shelf data augmentation method called "TrivialAugment" [47]. Again, we use an autoencoder with a CNN/DCNN architecture to embed each image:

Parameter	Value
Latent Size	128
Layers	5
Hidden Channels	8, 16, 32, 64, 128
Kernel Size	5
Stride	2
Activation Function	LeakyReLU(0.1) followed by BatchNorm

We train linear get/put models for the binary concept of "Smiling", resulting in a total of 1,071,749 parameters. The loss function is a weighted sum of the losses from each atomic task:

Hyper-parameter	Value	Task	Weight
Steps	100,000	AUTOENCODING	10
Batch Size	64	GETPUT	1
Optimiser	AdamW	PUTPUT	1
Learning Rate	10^{-3}	UNDO	1
Weight Decay	10^{-2}	PUTGET	1
Gradient Clipping	1 (element-wise)	CLASSIFICATION	1
Image Loss	$L_2 + 0.2 \cdot L_1 + SSIM$		
Value Loss	Binary cross-entropy		
Seed	0		

C.3 MNIST

We trained the `manipulator` pattern on the MNIST dataset, using the digit label as the property. The `get` operated directly on images, while `put` was trained to act on the latent space of an autoencoder, as in option (1) of Section 4.3. The images are input as 28×28 matrices, flattened to 784-dimensional vectors, and the labels are provided as 10-dimensional vectors with one-hot encoding. All of the components were structured as multilayer perceptrons. The hyperparameters are given below:

	enc	dec	put	get
Input Dimension	$784 = 28 \times 28$	32	$42 = 32 + 10$	$784 = 28 \times 28$
Output Dimension	32	$784 = 28 \times 28$	32	10
Hidden Dimensions	{128, 128, 64}	{64, 128, 128}	{128, 128, 128}	{64, 64}
Hidden Activations	ReLU	ReLU	ReLU	ReLU
Final Activation	Sigmoid	Sigmoid	Sigmoid	Softmax

With these architectural components, we trained four tasks: (a) training get supervised, (b) training get given pre-trained put, enc, and dec, (c) training put given pre-trained get', enc, and dec, and (d) training get to match a previous get'. These were trained using the manipulation rules, as well as PutPUT, and additional regularization term we denote as ENTROPY. The loss function of ENTROPY is given by

$$\mathcal{L}_{\text{ENTROPY}} = \mathbb{E}[H(\text{get}(\text{enc}(x)))] - H(\mathbb{E}[\text{get}(\text{enc}(x))])$$

where x is a batch of input images, $H(\cdot)$ is the entropy of a categorical distribution, and the expectation is approximated by the mean over each batch. The idea behind ENTROPY is to encourage the output of get to be well-distributed across labels (by maximizing the entropy of the mean distribution) but to be sure of each label (by minimizing the entropy for each specific input). For task (d), labels were generated for the CLASSIFY rule using get'. Each task is trained by minimizing a weighted linear combination of the rules. We give the hyperparameters, rule weights, and loss functions for each of these below.

	(a)		(b)		(c)		(d)	
Optimizer	Adam		Adam		Adam		Adam	
Learning Rate	0.001		0.001		0.0001		0.001	
Epochs	20		20		20		20	
	Weight	Loss	Weight	Loss	Weight	Loss	Weight	Loss
CLASSIFY	1	CE	–	–	–	–	1	CE
PUTGET	–	–	10	CE	10	CE	–	–
GETPUT	–	–	10	L2	10	L2	–	–
PUTPUT	–	–	10	L2	10	L2	–	–
UNDOABILITY	–	–	10	L2	10	L2	–	–
ENTROPY	–	–	1	$\mathcal{L}_{\text{ENTROPY}}$	–	–	–	–

We also have an additional task (e) of training enc and dec unsupervised. This was done using the Adam optimizer, with a learning rate of 0.001 for 80 epochs. The reconstruction loss was given by

$$\mathcal{L}(x, \hat{x}) = \text{L2}(x, \hat{x}) + (1 - \text{SSIM}(x, \hat{x}))$$

where SSIM is the structure similarity image metric.

To produce Figure 3, an enc, dec, put, and get were trained using (a) \rightarrow (e) \rightarrow (c), followed by training (c) for an additional 40 epochs. A slightly larger (but still MLP-based) model, where both put and get act on the latent space of the autoencoder, was used to achieve better visual quality. The hyperparameters are detailed below:

	enc	dec	put	get
Input Dimension	$784 = 28 \times 28$	32	$42 = 32 + 10$	32
Output Dimension	32	$784 = 28 \times 28$	32	10
Hidden Dimensions	{128, 128, 128, 32, 32}	{32, 32, 128, 128, 128}	{256, 256}	{256}
Hidden Activations	ReLU	ReLU	ReLU	ReLU
Final Activation	Sigmoid	Sigmoid	Sigmoid	Softmax

`enc`, `dec`, and `put` were used to manipulate six examples picked from the dataset, putting each of the ten classes onto each example. The examples were cherrypicked to provide maximum stylistic contrast across the sample but were not selected for maximum style transfer accuracy - a similar level was observed across the entire dataset. Code for all of these models, as well as the training schedules of tasks (a)-(e), are provided in the supplementary material.

D Examining Manipulation in complex domains

D.1 Manipulation for text sentiment

We attempted to fine-tune an extant strong solution for text-sentiment modification by additionally imposing the constraints of manipulation on top of the original objective function. Our findings suggest that **additionally imposing the constraints of manipulation on architectures that are already performant does not make an appreciable difference** (Table 1). We pretrained the Blind Generative Style Transformer (**B-GST**) model of [63] which takes in the non-stylistic components of a sentence and the target sentiment, and outputs the sentence generated in the target style. This was done until we achieved baselines higher than the original ones reported by the authors of the model. Afterwards, we continued training under three different conditions: (1) resuming training with only the original objective, (2) only using objective functions from manipulation, and (3) using both. For (1) and (3), we reused the same objective in the original paper. In all experiments, we used the YELP dataset used by [43], reusing the same train-dev-test split they used. It consists of 270K positive and 180K negative sentences for the training set, 2000 sentences each for the dev set, and 500 sentences each for the test set. Furthermore, we used the human gold standard references they provided for their test set. **B-GST** uses a sequence length of 512, 12 attention blocks each with 12 attention heads. We used 768-dimensional internal states (keys, queries, values, word embeddings, positional embeddings). We tokenized the input text using Byte-Pair Encoding (BPE).

We used the same input autoencoding and output decoding used in [63] across all experiments. For the `get` of the manipulation task, we used the PyTorch version of the pretrained Transformer by HuggingFace, which uses the OpenAI GPT model pretrained by [56] on the BookCorpus dataset which contains over 7000 books with approximately 800M words. We trained it on a sentiment classification task using the YELP dataset reaching 98% accuracy on the test set. The `get` was fixed for the entire duration of training conditions (2) and (3) above. For the `put` of manipulation, we used the **B-GST** model to generate text with a specified sentiment. This was a computational bottleneck for training conditions (2) and (3) as autoregressive decoding is required to generate model inputs for `PUTGET` and `UNDOABILITY` in manipulation. We used ‘teacher forcing’ or ‘guided approach’ [7, 70] whenever we computed the reconstruction loss of `put`. Additionally, for training conditions (2) and (3), we only used `PUTGET`, `GETPUT`, and `UNDOABILITY` from manipulation. We used a weighted sum of the losses computed for each of these and the original reconstruction loss if present - the weights can be considered as training hyperparameters. For (2), we used (`PUTGET`=5, `GETPUT`=20, `UNDOABILITY`=20), while for (3), we used (`PUTGET`=5, `GETPUT`=10, `UNDOABILITY`=25, `B-GST`=30). Code for all of the models, training schedules, and hyperparameter values for training conditions (1)-(3) are also provided in the supplementary material.

MODEL	GLEU	BLEU _{SRC}	BLEU _{REF}	ACC (FASTTEXT)
B-GST-pretrained	11.869	74.563	52.770	84.6
B-GST-only	11.426	74.876	52.549	85.7
manipulation-only	11.712	74.428	52.646	84.1
B-GST+manipulator	11.338	74.608	52.836	85.1
Human Reference	100.00	58.158	100.00	67.6

Table 1: We pretrained the Blind Generative Style Transformer (**B-GST**) model [63] based on the Delete-Retrieve-Generate [43] framework for sentiment modification until we recovered higher baselines than reported by the authors of the model (GLEU=11.6, BLEU_{SRC}=71.0), and we continued training in three different conditions: (1) keeping the original objective, (2) only using objective functions obtained from manipulation, and (3) using both. We report no statistically significant differences in scores, even under continued training. The table reports the results of training conditions (1) and (2) for an additional epoch, and (3) for two epochs.

D.2 Characterising Manipulation as generative classification

Training manipulation autoregressively (e.g. when instantiating the learners as transformers for sequential data) is slow due to autoregressing twice for PutPUT and Undoability. Moreover, our attempts to autoregressively manipulate the sentiment of IMDB reviews often resulted in a form of posterior collapse where put ignored the attribute and behaved as the identity function on text. Conceptually, this is because the identity function satisfies GETPUT, PutPUT and UNDOABILITY, and while the identity fails on PutGET, failing on one component of the combined loss function does not provide a strong enough incentive to move away from the identity in parameter-space.

Notably, these shortcomings mirror that of VAEs, which also suffer from posterior collapse [12] in highly structured domains such as video [3] and text [13]. This suggested to us that **puts may be generative classifiers, which could potentially explain why mode collapse was occurring in complex domains**. Borrowing terminology from [49], classifiers are *discriminative* if they seek to learn the conditional distribution $p(a|d)$ of attributes given data (as in the *classification* pattern), and otherwise they are *generative* if they seek to learn the joint distribution $p(d, a)$ (as, for example, a VAE). The tradeoffs between the two types are well studied, e.g. performance-wise, generative models may converge faster with limited data, but discriminative models often achieve lower asymptotic error, and it is well known that learning generative models is harder [66].

Manipulation cannot be viewed directly as a generative classifier, as the put admits extraneous conditionals on a reference and a target attribute. So we resorted to an empirical comparison of manipulation and VAEs as a known generative classifier; specifically, we compared their ability to approximate the Bayesian inverse, and we found their performance comparable. To demonstrate this, we tried three ways to train an "informationally identical" cls' given an initial cls , provided access to unlabelled data to obtain a distribution of pairs $(d, \text{cls}(d))$ by: (a) directly training cls by *classification*, (b) training a generative classifier, in our case a VAE, and (c) training manipulation around cls -as-get to obtain a put, and then train cls' to satisfy the tasks of manipulation except for *CLASSIFY*. Repeating this process several times, we would expect to see some loss of accuracy due to imperfect Bayesian inversion. Indeed, we see in Figure 8 that (b) and (c) have similar decays in accuracy, indicating that manipulation and VAEs have similar performance in this case. This experiment was performed using the trained components obtained from the MNIST experiment (Section C.3), and in addition to the tasks (a-e) we (f) trained a VAE to learn the joint distribution of images and labels produced by 'get', and we (g) trained a 'get' supervised using labels and images generated from the VAE. The VAE encoder and decoder are also based on multilayer perceptrons - each is comprised of an MLP trunk and two linear heads for generating the means and log-variances of the latent space, or the image and labels, respectively. The latent space is comprised of independent normally distributed variables as in [41], and is sampled using the standard reparameterization trick. The hyperparameters of the architecture are given below:

	VAE Encoder	VAE Decoder
Input Dimension	$794 = 28 \times 28 + 10$	32
Hidden Dimensions	{128, 128, 64}	{64, 128, 128}
Hidden Activations	ReLU	ReLU
Head 1 Dimension	32	$784 = 28 \times 28$
Head 1 Activation	–	Sigmoid
Head 2 Dimension	32	10
Head 2 Activation	–	Softmax

Three loss functions were used for tasks (f) and (g) — the reconstruction loss of the autoencoder, which can be separated into a label loss and an image loss, the K-L divergence regularization term \mathcal{L}_{KL} of the VAE [41], and the *CLASSIFY* loss of 'get'. The training hyperparameters are given as follows:

	(f)		(g)	
Optimizer	Adam		Adam	
Learning Rate	0.001		0.001	
Epochs	40		20	
	<i>Weight</i>	<i>Loss</i>	<i>Weight</i>	<i>Loss</i>
CLASSIFY	–	–	1	CE
Image Reconstruction	100	L2	–	–
Label Reconstruction	1	CE	–	–
K-L Divergence	0.5	\mathcal{L}_{KL}	–	–

In order to evaluate the three methods, we trained the tasks in the following order. At each step, the component being trained (e.g. `get`, `put`, etc) was initialized randomly (the previous weights were discarded). Measurements of the test accuracy were made after each (a), (b), (d), or (g) training run, and used to produce Figure 8.

$\text{get} \rightarrow \text{get}' \implies (\text{a}) \rightarrow (\text{d}) \rightarrow (\text{d}) \rightarrow \dots \rightarrow (\text{d})$
 $\text{get} \rightarrow \text{put} \rightarrow \text{get}' \implies (\text{a}) \rightarrow (\text{e}) \rightarrow (\text{c}) \rightarrow (\text{b}) \rightarrow (\text{e}) \rightarrow (\text{c}) \rightarrow (\text{b}) \rightarrow \dots \rightarrow (\text{b})$
 $\text{get} \rightarrow \text{VAE} \rightarrow \text{get}' \implies (\text{a}) \rightarrow (\text{f}) \rightarrow (\text{g}) \rightarrow (\text{f}) \rightarrow (\text{g}) \rightarrow \dots \rightarrow (\text{g})$

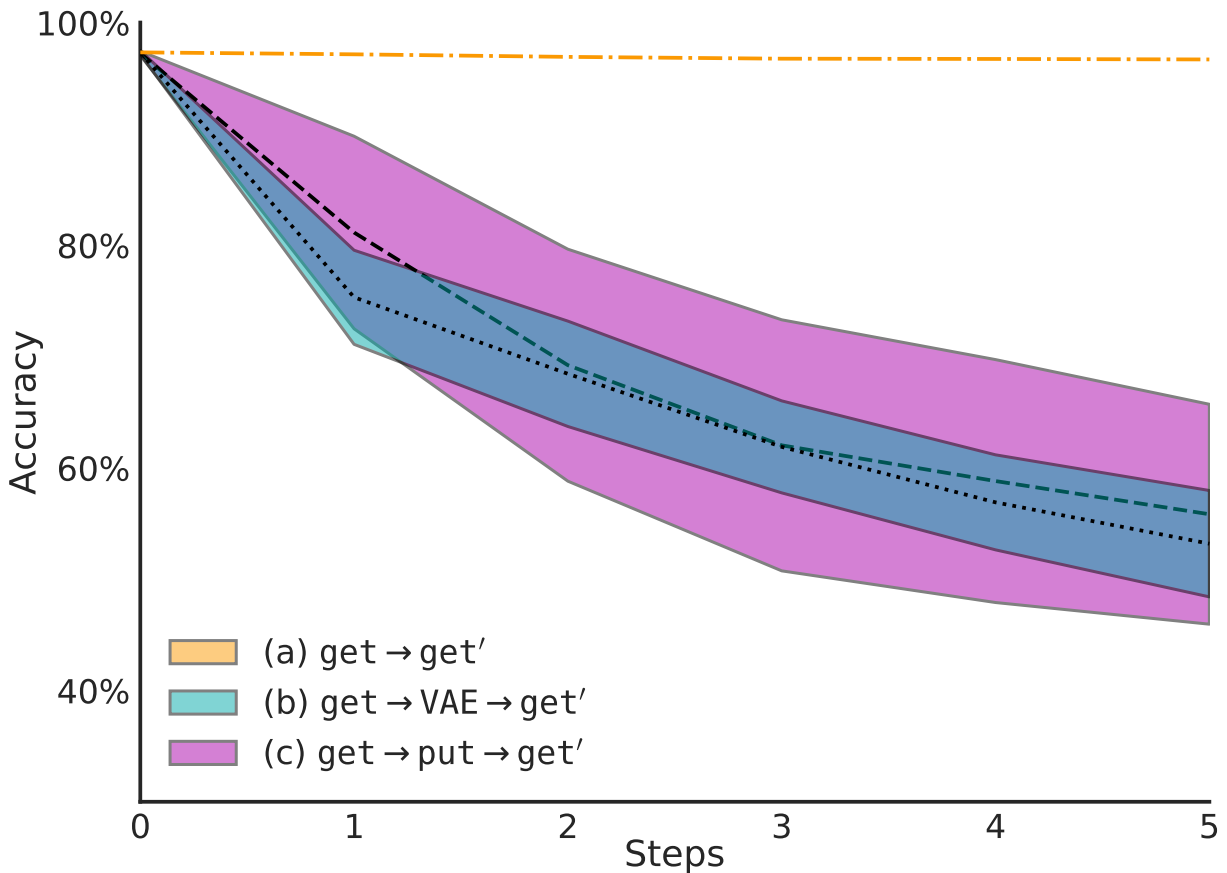


Figure 8: We tried three ways to train an "informationally identical" cls' given an initial cls - depicted are the results of training successive MNIST classifiers using methods (a), (b) and (c) given above. 'steps' refers to the number of times this process was repeated. We observe that the degradation of accuracy is approximately the same for both (b) and (c), **which we consider evidence that manipulator and VAEs have similar performance characteristics**. Both models had roughly the same number of parameters (300K) and were based on the same MLP architecture. We ran 20 repetitions of each method, the shaded regions represent one standard deviation (method (a) had a standard deviation of less than 1%).